Quantum phases of a bosonic generalization of the Moore-Read ansatz

Cameron James Richard Duncan

A thesis submitted to fulfill the requirements for the degree of Master of Philosophy
Faculty of Science, The University of Sydney

2019

Acknowledgements

I would like to acknowledge the encouragement and guidance of my supervisor, Professor Andrew Doherty, in helping me to complete this thesis. I would also like to thank my thesis examiners for making helpful recommendations on ways to improve the text.

Contents

1 Introduction to Spin-Moore-Read States

Tensor networks provide an accessible picture of the local structure of quantum entanglement and are thus a powerful tool in the investigation of quantum phases of matter. A key discovery of many-body quantum theory is that quantum states with finite correlation lengths do *not* all belong to the same quantum phase. This result is surprising, as one might have expected the entanglement of local degrees of freedom to vanish at spatial separations long compared to the correlation length. But there do exist states with finite correlation lengths that nevertheless possess non-local properties that distinguish their infrared (IR) fixed points from unentangled product states [40], [48]. Of particular interest are states of paramagnetic and magnet-like systems, more generally spin-lattices, such as can be engineered in optical traps or interacting quantum dots, among other settings. These systems are suspected to exhibit symmetry protected topological order (SPT) [10]. SPT phases are robust against local perturbations that respect privileged symmetries of the unperturbed Hamiltonian. The characteristic features of SPT phases are massive bulk and massless edge excitations; SPT phases are therefore the interacting generalization of topological band insulators [3]. Cohomology of physical symmetries furnishes a classification of bosonic SPT phases [11], akin to a periodic table, a result also expressable in the language of tensor-networks [50]. A present task for theorists is to fill out the as yet unknown details of this table by identifying trial wavefunctions that (a) belong to non-trivial SPT phases and (b) are amenable to concrete calculations. The goal of this thesis is to show how tensor networks can be applied to carry out this task systematically.

The focus of this thesis is one particular family of trial wavefunctions. These wavefunctions are the adaption to the bosonic case of a construction first proposed by Moore and Read (MR) as a class of ansatz for interacting fermions in two dimensions [33]. An *MR wavefunction* equates the first-quantized amplitudes of the trial wavefunction with the conformal blocks of a Conformal Field Theory (CFT). Motivating the MR proposal is the formal similarity between the data that define, on the one hand, a CFT and, on the other, a system of quasiparticles. Conformal blocks are multi-valued complex functions of n space-time coordinates that serve as convenient basis functions for expanding CFT n-point correlators. The abstract labels that distinguish the branch cuts of a conformal block play the role of topological quantum numbers for MR states.

A natural extension of MR's idea is to consider many-body wavefuctions built in much the same way from two-dimensional-CFT correlation functions. These *Spin MR states* (MR-like states of spin lattices) are single valued in particle coordinates and thus do not carry the topological quantum numbers that motivate investigations of MR-states. Instead, Spin MR-states are of interest because (a) characterizing their phases is an open problem and (b) because there is convincing numerical evidence that particular examples exhibit SPT order.[41]

Spin MR-states take the form,

$$|\Psi\rangle := (\text{f.c.}|\, T\left\{\exp\left[\int_S d^2x\ \phi(\mathbf{x}) \otimes a^\dagger(\mathbf{x})\right]\right\} |\text{i.c.})\, |00\ldots0\rangle\,. \tag{1}$$

Here, $|00\ldots0\rangle\,,\ |\Psi\rangle \in \mathcal{H}$ are states of a lattice of spins (i.e., local degrees of freedom) with $|00\ldots0\rangle$ the all-up state, whereas $|\text{i.c.}),\ |\text{f.c.}) \in \mathcal{V}$ are initial and final states (conditions) in the distinct Hilbert space of a CFT [19]. The expression $T\{\exp[\ldots]\}$ denotes an imaginary-time ordered exponential. The operator valued function $a(\mathbf{x})$ is the lowering operator on the spin lattice and $\phi(\mathbf{x})$ is a primary field in the CFT. The body of this thesis frequently refers back to Eq. (1), because it defines our object of study. The roles played by $\mathcal{H}$ and $\mathcal{V}$ on the right-hand-side of Eq. (1) resemble those of the *physical* and *virtual* indices of a tensor network, and thus these states readily invite a local tensor network decomposition, in contrast to the non-local decomposition that proves useful in the study of fermionic MR-states (as shown, for example, in [53]).

Spin-MR states represent just one among other possible ideas for generalising the Moore-Read construction to bosonic wavefunctions. Specifically, there exist conformal blocks that transform evenly on permuting holomorphic space-time coordinates, and the more immediate generalisation is to identify these conformal blocks with states of bosonic particle ensembles. Such wavefunctions are appropriately categorized as MR states, because they are suitable trial wavefunctions for the FQHE at even filling (the ratio of electrons to fluxons is even) and other phenomena that involve charged bosons in the presence of high magnetic fields [26]. The choice of conformal blocks and not correlation functions, as in Eq. (1), has the consequence that the boundary excitations implied by a bulk-boundary correspondence are chiral, meaning that they have a preferred direction of propagation. MR states for bosonic FQHEs are investigated in detail in a series of papers by Siera, Nielsen, Cirac and coworkers, including [34] and [20]. Chiral edge excitations imply the absence of time-reversal symmetry and thus these states are not candidates for SPT wavefunctions. To draw connections between the methods developed in this thesis for studying non-chiral Spin-MR states and the study of their chiral analogs is outside my scope, but a suitable topic for future work.

Spin MR states are largely unstudied in the many-body quantum literature. The lack of attention speaks more to the success of non-interacting topological band theory in explaining experimental results (see, for example, [54]). It is plausible that experiments will find topological-insulating behavior in which interactions do play an important role, much as the fractional quantum hall effect (FQHE) cannot be explained by non-interacting theory. Placing in context the results of this thesis, [41] is the only work known to the author to investigate whether Spin-MR states might exhibit SPT order. The authors of [41] begin with wavefunctions that belong to SPT phases by construction and from there compute numerical evidence that these wavefunctions are also Spin-MR states (i.e., are expressible in the

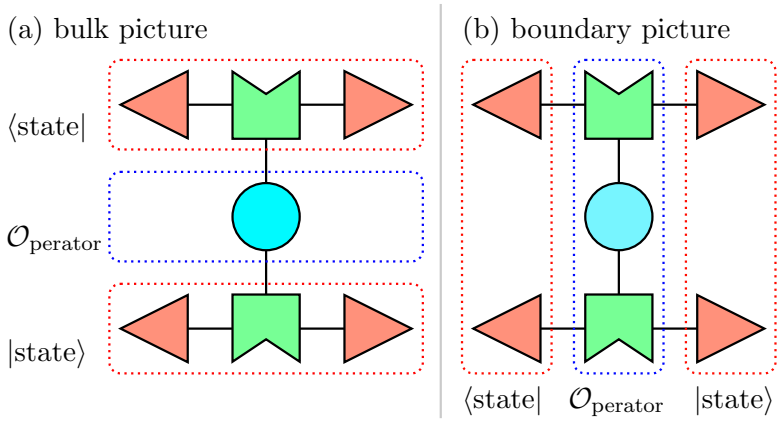

Figure 1: Holographic correspondence between bulk and boundary pictures; solid figures represent tensors and solid lines tensor indices; let:

- the red triangles be v^i;
- the green badges be $A^{ij}{}_k$; and,
- the blue circle $X^i{}_j$;

dotted lines enclose particular sub-networks interpreted as state and operator; joining two solid figures by a solid line represents index contraction; the identical networks shown in sub-figs. (a)-(b) represent an expectation value;

Sub-fig. (a), the bulk picture: collecting the factors as $(v^*_n A^n{}_{\ell m} v^m)^* X^\ell{}_k (v^*_j A^{jk}{}_i v^i)$, the factors in round-brackets are the quantum state and its dual, the remaining factor the operator. Translated from algebra to diagram, the bottom-most sub-network, enclosed by the red dotted line, is identified as the state and the topmost its dual, as indicated by horizontal reflection; the red shaded triangles are boundary conditions on the bulk degrees of freedom represented by the green badge; the blue circle is an observable acting on the bulk degrees of freedom;

Sub-fig. (b), the boundary picture: collecting the factors as $(v^i v^{*m})(A^{jk}{}_i X^\ell{}_k A^{*n}{}_{\ell m})(v^*_j v_n)$, the first and last factors enclosed in brackets are the dual and the state, the remaining factor the operators, so that, in the figure, the left-most sub-network is identified as the state, and the right-most its dual.

form (1) with respect to the partition function of a CFT.) This thesis approaches the relationship between SPT phases and Spin-MR states from the opposite direction. Beginning with an explicit tensor network description of Spin-MR states, I compute a signature that these states belong to non-trivial phases, namely, bipartite entanglement spectra, formally introduced in Chapter 3.

Tensor networks enter as a tool for computation and physical interpretation of many-body systems [45]. Tensor networks are useful because they make manifest holographic dualities, such as are described in [12]. This thesis is interested in the form of tensor-network holography shown in Fig. (1): namely, with respect to any patch of the two-dimensional surface on which the Spin MR-State lives, there is a correspondence between (i) states of the degrees of freedom in the interior, or bulk, of the patch and (ii) the different boundary conditions that may be imposed on the patch. The correspondence is a consequence of the physical arbitrariness inherent in distinguishing states from operators, granted the premise that the only physically meaningful quantities in a quantum theory are expectation values of observables. To elaborate: when an expectation value is expressed as a tensor network, there is an arbitrary choice as to which sub-network is identified as the state and which the operator. This holographic correspondence is to space what the more familiar equivalence between Schrodinger and Heisenberg pictures is to time. The holographic correspondence allows us to identify fixed point wavefunctions belonging to the same phase as our Spin-MR states, using the technology of boundary-CFT and following the techniques applied to fermions in [15]. In this way, our original 2D network reduces to a 1D spin chain, making tractable the calculation of expectations values of co-linear local operators and entanglement spectra along boundaries with one component.

The bulk-boundary correspondence just described implies a formal equivalence between equal-time correlation functions of Spin-MR states and general n-point correlators of a $1+1D$ CFT. This equivalence makes it possible to formulate conditions under which the correlation length of a spin-MR state is finite. A spin-MR state is characterized by the choice of CFT operator ϕ appearing in Eq. (1). The conformal weight of ϕ plays the role of inverse temperature for the particle ensemble and there is a Kosterlitz-Thouless phase transition between finite and infinite correlation length at a critical value of the conformal weight. These notions can be made precise in reference to the particular examples considered in Chapter 2, which motivate the techniques developed in Chapters 3, 4 and 5.

Chapter 3 shows that the bulk-boundary picture makes possible a continuum boundary-picture approximation of a bulk wavefunction defined on a lattice. The approximate continuum theory is a locally perturbed CFT, a class of model that is suitable for study by renormalisation-group (RG) methods, as in [8], [2].

The main results of the thesis come in Chapters 4 and 5. Chapter 4 presents an algorithm that takes the ground-state of the approximate boundary theory as input and yields the entanglement spectrum of the bulk state as output. Chapter 5 applies this algorithm to

states with finite correlation length and shows how to calculate the low-energy sector of the entanglement spectrum via techniques of Boundary CFT. This use of Boundary CFT relies on identifying massive fixed points of the RG flow away from the unperturbed CFT with conformal boundary conditions on the CFT [8].

The results of this thesis are a point of departure for a numerical research program, in two ways. First, the algorithm presented in Chapter 4 structures a future numerical search for signatures of SPT ordered Spin-MR states in the space of CFTs. Second, the approximations in Chapters 3, 4 and 5 provide analytical tools for interpreting numerical results. There is a need for such tools, because the higher-dimensional objects involved in tensor network numerics necessitate lower-dimensional numerical approximations (see [16], [35] and [1]) that are in practice opaque and therefore error-prone. The approximations in Chapters 3 and 4 are shown to be exact in the dilute limit, in which particle density vanishes on the lattice scale. The results of Chapter 5 are exact in the limit of vanishing correlation length. Altogether, therefore, the analytically tractable approximation developed by the end of the thesis is exact in the limit that particle density is (a) small on the lattice scale but (b) large on the scale of the system size. By starting numerics in the large, dilute limit, and cross referencing analytical calculations, the physics beyond the regime of approximation can be explored numerically with greater confidence.

2 Ising model Spin-Moore-Read states

The purpose of this chapter is to make the definition of Spin-MR states concrete with reference to simple examples. These examples have not been investigated in earlier literature. I derive clues that motivate the detailed calculation of entanglement spectra in Chapters 4 and 5. I find Spin-MR states with finite correlation lengths (i.e., belonging to a massive phase) and infinite (massless phase). Finite correlation length is a necessary condition for SPT order: thus, some Spin-MR states do not correspond to SPT phases. I make an incomplete investigation of the phase-space neighbourhood of my massive examples, locating some critical points but not entire phase boundaries. Deciding whether an arbitrary wavefunction $|\Psi\rangle$ is SPT ordered is intractable and thus an important research question is whether there are probative yet easily computed probabilistic tests of SPT order. Strange-correlators — correlation functions for which the in-state is not dual to the out-state — are a proposed diagnostic of SPT order [52]. An immediate consequence of the Spin-MR construction is that strange correlators of Spin-MR States with the Fock-vacuum necessarily decay algebraically.

2.1 First examples: Spin-operator Spin-Moore-Read states

Our first motivating examples of Spin-MR states choose the critical Ising model in two dimensions as the auxiliary CFT and the Ising spin operator σ as the field ϕ appearing in Eq. (1). States of individual physical spins, $\{|0\rangle, |1\rangle\}$ in the Pauli Z basis, are given a lattice-gas interpretation: $|0\rangle$ signifies the absence and $|1\rangle$ the presence of a particle at the corresponding lattice site. Labeling basis vectors in the Z product basis by the locations $\{\mathbf{x}_i\}$ of the $|1\rangle$ factors (the particles), our non-normalized Spin-MR wavefunction is,

$$\langle \{\mathbf{x}_i\}_{i\leq n} \mid \Psi\rangle := \mu^n \langle \sigma(\mathbf{x}_1) \dots \sigma(\mathbf{x}_n)\rangle \,, \tag{2}$$

where μ is a fugacity parameter (inserted to make the wavefunction amplitude fall exponentially with total particle number). The presence of the fugacity parameter is the reason for the plural "examples" in the title of this subsection. By way of comparison, Levin and Gu construct an SPT-odered wavefunction, having global Pauli Z symmetry, for this spin-lattice in [29].

If the examples parameterized by Eq. (2) are really to be motivational then there ought to be surface-level reasons for suspecting that some values of μ are in a massive, non-trivial quantum phase. There are two especially tractable limits: $\mu \to 1$ and $\mu \to 0$.

2.1.1 The limit $\mu \to 1$

For $\mu = 1$, $|\Psi\rangle$ as defined in Eq. (2) has a simple expression in the Pauli X basis, without any reference to the Hilbert space of the auxiliary CFT. Let Pauli X eigenstates be labeled,

$$|+\rangle := \frac{1}{\sqrt{2}}\left(|0\rangle + |1\rangle\right), \quad |-\rangle := \frac{1}{\sqrt{2}}\left(|0\rangle - |1\rangle\right), \tag{3}$$

and let the spin lattice have N sites. Then, I claim,

$$|\Psi\rangle = \frac{\mathcal{N}}{2^{N/2}} \sum_{\{X_i\}} \exp\left[\beta_c \sum_{\langle p,q\rangle} X_p X_q\right] |\{X_i\}\rangle \tag{4}$$

$$= \mathcal{N} \exp\left[\beta_c \sum_{\langle p,q\rangle} X_p X_q\right] |0\rangle\,. \tag{5}$$

Here β_c is the critical temperature of the 2D classical Ising model, $\Sigma_{\{X_i\}}$ denotes the sum over all product states in the Pauli X basis, and $\mathcal{N}$ is a constant of proportionality to be calculated shortly. Equation (5) follows from Eq.(4) by inverting Eqs. (3). To see that Eq. (4) is equivalent to Eq. (2) setting $\mu = 1$, compute the overlap in the $|\{\mathbf{x}_i\}\rangle$ basis:

$$\begin{aligned}
&\frac{\mathcal{N}}{2^{N/2}} \langle\{\mathbf{x}_j\}_{j\le n}| \sum_{\{X_i\}} \exp\left[\beta_c \sum_{\langle p,q\rangle} X_p X_q\right] |\{X_i\}\rangle \\
=&\frac{\mathcal{N}}{2^{N/2}} \langle 0| \prod_j^n X_j \sum_{\{X_i\}} \exp\left[\beta_c \sum_{\langle p,q\rangle} X_p X_q\right] |\{X_i\}\rangle \\
=&\frac{\mathcal{N}}{2^{N}} \sum_{\{X_k\}} \sum_{\{X_i\}} \langle\{X_k\}| \prod_j^n X_j \exp\left[\beta_c \sum_{\langle p,q\rangle} X_p X_q\right] |\{X_i\}\rangle \\
=&\langle \sigma(\mathbf{x}_1) \ldots \sigma(\mathbf{x}_n)\rangle\,,
\end{aligned} \tag{6}$$

assuming the constant $\mathcal{N}$ is set to the value,

$$\mathcal{N}^{-1} = \langle 0| \exp\left[\beta_c \sum_{\langle i,j\rangle} X_i X_j\right] |0\rangle\,. \tag{7}$$

The operator exponential (Gibbs operator) in Eq. (5) has a refection symmetry $X \mapsto ZXZ = -X$ for which X is the order parameter. The state $|\Psi\rangle$ is disordered with respect

to X and it follows immediately from Eq. (4) that,

$$\langle\Psi|\, X_p X_q \,|\Psi\rangle = \frac{\mathcal{N}^2}{2^{2N}} \sum_{\{X_k\}} \sum_{\{X_\ell\}} \langle\{X_k\}|\, X_p X_q \exp\left[2\beta_c \sum_{\langle i,j\rangle} X_i X_j\right] |\{X_\ell\}\rangle \tag{8}$$

$$= \frac{\mathcal{N}^2}{2^{2N}} \sum_{\{X_k\}} X_p X_q \exp\left[2\beta_c \sum_{\langle i,j\rangle} X_i X_j\right], \tag{9}$$

where the sum in Eq. (9) is taken over classical configurations. Thus, $|\Psi\rangle$ has finite correlation length equal to that of the classical 2D Ising model at inverse temperature $\beta = 2\beta_c$. The two trivial disordered states with respect to the same order parameter are $|0\rangle$, $|1\rangle$.

The question of quantum phase is thus: do there exist local deformations that commute with Z and take $|\Psi\rangle \mapsto |0\rangle, |1\rangle$, but without the correlation length diverging at some point along the path in Hilbert space? Attempting to answer this question, it is helpful to generalize the form of Eq. (5) to,

$$|\Psi', \boldsymbol{\eta}\rangle := \frac{e^{-\beta H(\boldsymbol{\eta})}}{\langle\alpha|\, e^{-2\beta H(\boldsymbol{\eta})} \,|\alpha\rangle} |\alpha\rangle, \tag{10}$$

where $|\alpha\rangle$ lives in the *same* Hilbert space as $|\Psi\rangle$. The $\boldsymbol{\eta}$ abstractly parameterizes the couplings in the Hamiltonian H. The form of the definition of $|\Psi'\rangle$ resembles the definition of Spin-MR states in Eq.(1), except that the auxiliary degrees of freedom have been traced out. A second, subtler difference is that the Gibbs-operator in Eq. (10) is positive definite (the H operator is Hermitian) but the exponential in Eq. (1) is not. It is therefore not possible to calculate an expression of the form in Eq. (10) from Eq. (1) by brute force computation of the auxiliary expectation value appearing in Eq. (1). A systematic procedure for re-expressing a Spin-MR state in terms of the action of a *unitary operator* on a generalised vaccum state might be found by exploring the parallels with *continuous* tensor networks as proposed in [25], but these parallels are not pursued here. The fact the Hamiltonian in the expression for $|\Psi\rangle$ in Eq. (5) is the same as the Hamiltonian in the auxiliary CFT is only possible because the dimensions of the local Hilbert spaces (auxiliary and physical) are equal. If the auxiliary space of the Spin-MR State has a greater number of local dimensions than the physical Hilbert space, then one expects the Hamiltonian in Eq. (10) to include non-local interaction terms. An important feature of Eq. (10) is that the normalisation factor appears as a classical partition function at 2β. Hence, if β is taken to be a classical critical inverse temperature, the two point functions of operators that commute with $H(\boldsymbol{\eta})$ will be related to statistical mechanical two-point functions *colder* than the critical temperature.

In the formalism of Eq. (10), $|\Psi\rangle = |\Psi', \boldsymbol{\eta}_0\rangle$ with $H(\boldsymbol{\eta}_0) = H_0$ the Ising model Hamiltonian in Eq. (5) at $\beta = \beta_c$. We seek a path through $\boldsymbol{\eta}$ space that ends at $|\Psi', \boldsymbol{\eta}_1\rangle = |0\rangle$. Let us

first consider paths in $\boldsymbol{\eta}$ space such that $[H(\boldsymbol{\eta}), H_0] = 0$. A divergence in correlation length at intermediate $\boldsymbol{\eta}$ is then inevitable, because the path can be mapped onto the phase space of the classical 2D Ising model. The Z symmetry protection confines the phase space path to the line $h = 0$, h the applied magnetic field. The two point expectation value $\langle \Psi' | X_i X_j | \Psi' \rangle$ begins at the classical inverse temperature $\beta = 2\beta_c$. The two point expectation at the destination is taken with the classical inverse temperature $\beta = 0$. Hence, the two point expectation must pass through the classical critical temperature, where the correlation length diverges.

By introducing terms to H in Eq. (10) that do not commute with H_0, $|\Psi'\rangle$ leaves the classical phase space. The only local term allowed by symmetry is $\mu' Z$, with μ' parametrising the strength of the coupling. Near $\mu' = 0$, there is an explicit functional relationship between μ' and the fugacity μ appearing in Eq. (2), which the next paragraph shows. The deformed Hamiltonian in Eq. (10) is then the quantum 2D transverse field Ising model, which is an anisotropic 3D classical model. In the limit that $\mu' \to \infty$, $|\Psi'\rangle = |0\rangle$. The 2D transverse field Ising model encounters a phase transition at critical value of $\mu' \in (0, \infty)$ [44]. Hence, at $\mu = 1$ in Eq. (2), the two most obvious paths in Hilbert space from $|\Psi\rangle$ to the trivial disordered state $|0\rangle$ encounter a point of diverging correlation length. Hence, there is reason to suspect that Eq. (2) at $\mu = 1$ might be SPT ordered with respect to global Pauli Z.

Returning to the definition of $|\Psi\rangle$ in Eq. (2), now consider $\mu \sim 1$. At any μ, a similar calculation as led to Eq. (6) also leads to,

$$|\Psi\rangle = \mathcal{N} \left(\frac{\sqrt{\mu}}{2} \right)^N \exp \left[- \ln \sqrt{\mu} \sum_i Z_i \right] \exp \left[\beta_c \sum_{\langle i,j \rangle} X_i X_j \right] |0\rangle \,, \tag{11}$$

with the factor $\mathcal{N}$ again given by Eq. (7) and N the number of lattice sites. To linear order in $\mu' = (\mu - 1)/2$, therefore,

$$|\Psi\rangle \propto \exp \left[\beta_c \sum_{\langle i,j \rangle} X_i X_j - \mu' \sum_i Z_i \right] |0\rangle \,, \tag{12}$$

giving the expression for $|\Psi\rangle$ near $\mu = 1$ without reference to the auxiliary CFT. Introducing $\mu \neq 1$ means that at quadratic order and higher in μ' the coefficients of $|\Psi\rangle$ in the Pauli X basis are no longer classical Boltzmann weights.

A last question asked of the $\mu \to 1$ limit in this chapter is how close $\mu = 1$ comes to a particle-site occupation probability of one-half. The occupation probability $p(i)$ of site i is,

$$p(i) = \frac{1 - \langle \Psi | Z_i | \Psi \rangle}{2}, \tag{13}$$

and hence half-filling corresponds to $\langle\Psi|\, Z_i\, |\Psi\rangle = 0$. At $\mu = 1$, Z_i acts on $|\Psi\rangle$ to change the sign of X_i in the Gibbs-operator appearing in Eq. (5). The quantum expectation value can therefore be equated with the following classical expectation value,

$$\langle\Psi|\, Z_i\, |\Psi\rangle \Big|_{\mu=1} = \left\langle e^{-2\beta_c \sum_{j=0}^{3} X_i X_j} \right\rangle_{\text{Ising, } \beta=2\beta_c}, \tag{14}$$

where the expectation on the right-hand-side is with respect to the 2D classical model at inverse temperature $2\beta_c$. The sum is over the nearest neighbours to site i. An assumption good at low temperatures is that the probability of finding all spins in this cluster aligned is unity, hence $\langle\Psi|\, Z_i\, |\Psi\rangle \approx e^{-8\beta_c}$ and $|\Psi\rangle$ is half-filled to within a few percent. An approximation to $|\Psi\rangle$ that is exactly half-filled and respects the Z symmetry is therefore,

$$|\Psi\rangle \sim \frac{1}{\sqrt{2}}(|+\rangle^{\otimes N} + |-\rangle^{\otimes N}), \tag{15}$$

the quantum superposition of the two ferromagnetic ground states of the classical model. The expression Eq. (15) is the result of taking the $\beta \to \infty$ limit in Eq. (10).

I conclude the discussion of the $\mu \to 1$ limit of Eq. (2) by relating it to a previously investigated tensor network ansatz. Verstraete *et al.* in [46] consider all states $|\psi\rangle$ such that there exists a local classical partition function Z_ψ and the coefficients (in some basis) of $|\psi\rangle$ are the Boltzmann weights of $Z_\psi(\beta < \frac{1}{2}\beta_c)$. They show that all such $|\psi\rangle$ are representable as *Projected Entangled Pair States*, a class of tensor networks, and, moreover, that for each $|\psi\rangle$ there exists a local, massive Hamiltonian such that $|\psi\rangle$ is the ground state. They present the assumption that $\beta < \frac{1}{2}\beta_c$ as essential to their derivation that a PEPS representation exists (recall Eq. (4) has $\beta = \beta_c$ for the Spin-MR state).

2.1.2 The limit $\mu \to 0$

To higher than linear order in $\ln \mu$, the H in Eq. (10) contains additional terms, given from Eq. (11) by the Baker-Campbell-Hausdorff formula. Rather than compute the coefficients of these terms, a cleaner approach is to sum Eq. (2) in powers of μ. A closed form expression for the *square* of non-vanishing $2n$-point spin-spin correlation functions gives the probability densities [13],

$$|| \langle \{\mathbf{x}_i\}_{i\leq n} \mid \Psi\rangle ||^2 = \mu^{2n} \langle \sigma(\mathbf{x}_1) \dots \sigma(\mathbf{x}_{2n}) \rangle^2 \tag{16}$$

$$= \frac{\mu^{2n}}{2^n} \sum_{\epsilon_i \pm 1,\ \Sigma\epsilon_i = 0} \exp\left\{ \sum_{i<j} \frac{\epsilon_i \epsilon_j}{2} \ln ||\mathbf{x}_i - \mathbf{x}_j|| \right\}. \tag{17}$$

The exponential terms on the right-hand-side of Eq.(17) each look like Boltzmann weights of a two-component plasma, a *Coulomb gas*. The outer sum makes the probability density

symmetric with respect to permuting the charges of individual particles, ensuring that the plasma is neutral. The mathematical equivalence of Spin-MR States and multi-component plasma is a coincidence of the free-space Green's function of the Laplacian in two dimensions:

$$\nabla^2 \ln ||\mathbf{x} - \mathbf{y}|| = 2\pi\delta^2(\mathbf{x} - \mathbf{y}). \tag{18}$$

This Green's function implies Boltzmann weights that decay algebraically with charge separation, hence behaving like the n-point correlators of a CFT. The plasma analogy offers an intuitive way to reason about the universal features of $|\Psi\rangle$, but because CFT correlators decay algebraically in all dimensions, the plasma analogy only holds in two-dimensions.

MR proposed interpreting the square norm of MR states as the partition function of a multi-component plasma: from this interpretation they argue for a finite correlation length from the assumption that the plasma is in its screening phase. With respect to our Ising spin MR-state, it is possible to defend the screening assumption by identifying $\langle\Psi|\Psi\rangle$ with the perturbative expansion of a solvable, massive model. The formula in Eq. (17) is a consequence of mapping the product of two Ising models onto a Gaussian theory, namely, the orbifold boson, in which the dynamical variable φ only takes distinct values in the unit interval: [13],

$$\langle\sigma(\mathbf{x}_1)\dots\sigma(\mathbf{x}_{2n})\rangle^2 = \left\langle \prod_{i=1}^{2n} \sqrt{2}\cos\left[\varphi(\mathbf{x}_i)/2\right] \right\rangle_{\varphi}. \tag{19}$$

Hence, $\langle\Psi|\Psi\rangle$ is *perturbatively* the same Gaussian model plus an interaction term $\mu\cos\varphi(x)$ in the action. The small parameter in the perturbation series is the fugacity μ of the particle ensemble, which enters at order equal to the number of particles. To be more explicit, referring back to the probability densities defined in Eq. (2), the squared norm is, to order $2n$ in the fugacity,

$$\begin{aligned}
\langle\Psi|\Psi\rangle &= \sum_{j=2}^{2n} \frac{1}{j!} \int dx_1 dy_1 \dots \int dx_j dy_j || \left\langle \{\mathbf{x}_i\}_{i\le j} \mid \Psi \right\rangle ||^2 + \mathcal{O}\left(\mu^{2(n+1)}\right) && (20)\\
&= \left\langle \sum_{j=2}^{2n} \frac{\mu^j}{j!} \int dx_1 dy_1 \dots \int dx_j dy_j \prod_{i=1}^{j} \sqrt{2}\cos\left[\varphi(\mathbf{x}_i)/2\right] \right\rangle_{\varphi} + \mathcal{O}\left(\mu^{2(n+1)}\right) && (21)\\
&= \left\langle \exp\left\{ \int\int dxdy\ \mu\sqrt{2}\cos[\varphi(\mathbf{x})] \right\} \right\rangle_{\varphi}, && (22)
\end{aligned}$$

where Eq. (22) defines a perturbed partition function.

If, on the right hand side of Eq. (22), we ignore the gauge redundancy in computing the expectation value introduced by orbifolding, then the perturbed action is a particular phase

of Sine-Gordon (SG) model, which is conventionally expressed [21],

$$S = \int d^2x \frac{1}{2} (\nabla\phi)^2 + \frac{z}{a}\cos(\beta\phi), \tag{23}$$

where $\phi = \varphi/(2\sqrt{\pi})$. Our partition function equivalent to $\langle\Psi|\Psi\rangle$ has parameter value $\beta^2 = \pi$ and thus belongs to the massive SG phase, the transition to the massless phase occurring at $\beta^2 = 8\pi$. Therefore, in the small μ limit, there is good evidence that local correlations of $|\Psi\rangle$ decay exponentially.

2.2 Ising operators other than spin

A second set of Spin MR states are realized by Ising model correlators if ϕ in Eq. (1) is chosen to be the energy density operator ϵ. The energy density operator is defined as the leading term in the local expansion of the product $\sigma(\mathbf{x})\sigma(\mathbf{y})$ in the limit $\mathbf{y} \to \mathbf{x}$. The n-point correlators of the energy density are equivalent to the expectation of the kinetic term in the Gaussian model [13],

$$\langle\epsilon(\mathbf{x}_1)\dots\epsilon(\mathbf{x}_n)\rangle^2 = \left\langle \prod_{k=1}^{p} [\nabla\varphi(\mathbf{x}_k)/2]^2 \right\rangle_{\varphi}. \tag{24}$$

Thus, the same reasoning that leads to Eq. (22) also implies that this new square norm $\langle\Psi|\Psi\rangle$ is the partition function for a *massless* free scalar field. The fact that the correlation length is finite for a Spin MR state constructed from σ but infinite constructed from ϵ is an example of a Kosterlitz-Thoules (KT) transition [28]. The KT transition in a Coulomb gas takes place at a critical value of the charge-to-temperature ratio. The plasma-like expression of the probability density Eq. (17) means that the electric charge on the plasma side of the analogy maps over to the exponent of the algebraically decaying two-point correlator on the CFT side. In CFT jargon, this exponent is the *conformal weight* of the field operator. The conformal weight of σ is $h, \bar{h} = 1/16$ whereas for ϵ it is $h, \bar{h} = 1/2$, and so the effective charge to temperature ratio q^2/kT for the σ ensemble is $1/2$ and for the ϵ ensemble 4: the KT transition takes place at the KT point $q^2/kT \approx 2$ [28]. The ϵ Spin-MR state is in a massless phase and therefore cannot be of interest as an SPT trial wavefunction. The lessons are as follows. Not all Spin-MR states are SPT ordered. In order to obtain an SPT trial wavefunction, the conformal weight of the primary field ϕ must be chosen sufficiently small (ϕ here having the same meaning as in Eq. (1)).

2.3 Strange correlators and the protecting symmetry

Interpretation of SPT inner-products as partition functions has gained attention as a diagnostic tool due to the following result first shown by You et al. in [52]. If $|\Psi\rangle$ is an SPT

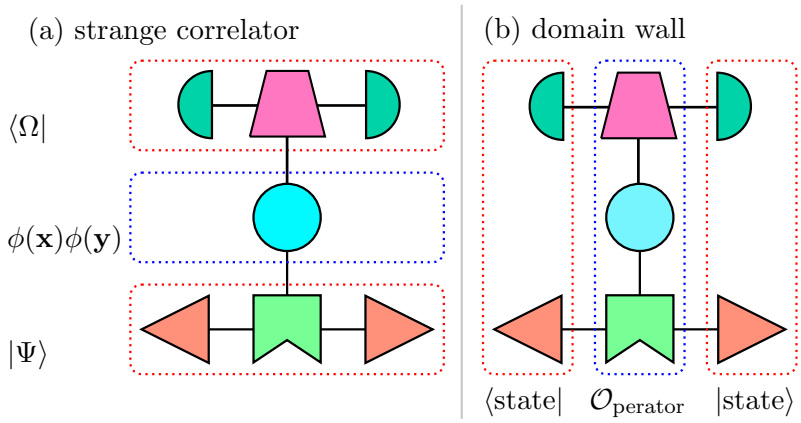

Figure 2: A space-like strange-correlator in the bulk picture (a) is a time-like correlation function at a domain wall in the boundary picture (b) (solid shapes and lines represent tensor contractions, as in Fig 1).

ordered state and $\langle 0|$ is a product state invariant under the protecting symmetry, then,

$$Z[J] = \frac{\langle 0| \, e^{\int dx^2 JX} \, |\Psi\rangle}{\langle 0|\Psi\rangle}, \tag{25}$$

is either a critical or symmetry breaking partition function for some order parameter X. The authors exchange the roles of space and time as shown in Fig. 2.3 and argue that the criticality of the partition function is preserved under the transformation. The exchange takes the space-like correlation function between two boundaries in time (in-states and out-states) to a time-like correlation function between two boundaries in space (asymptotic boundary states on either side of a domain wall) (see also [43]). The definition of SPT order implies that the physics at a spatial boundary between an SPT ordered state with a trivial state respecting the same symmetry must be described by a critical partition function. Criticality of the Z in Eq. (25) is implied by the algebraic decay of the two-point "strange correlator" $\langle 0| \, X(x)X(y) \, |\Psi\rangle$. Researches have used quantum monte-carlo and the strange correlator to find numerical evidence of SPT phase transitions for 1D and 2D spin lattices [49], [51].

If $|\Psi\rangle$ is a Spin-MR state and $|0\rangle$ the lattice gas vacuum, then $\langle 0|\Psi\rangle$ is critical, because the inner product is by construction the partition function for the CFT that defines $|\Psi\rangle$. That is, the strange-correlator diagnostic provides evidence that *all* Spin-MR states are SPT ordered. Nonetheless, we have already seen examples of Spin-MR states that are not SPT ordered. These Spin-MR states therefore show that the strange-correlator diagnostic is fallible.

2.4 'Edgeability' and other diagnostics of SPT order

Ryu and coworkers recently proposed a CFT-based diagnostic of SPT order in 2+1D that pertains to the Spin-MR construction [22] (and see further [6]). Namely, if the SPT ordered state lives on a disc, then the 1+1 CFT that emerges on the circular edge cannot be defined on a line-segment consistent with the protecting symmetry. This statement amounts to the claim that any boundary conditions, except free boundary conditions, imposed at the endpoints of the line segment must break the protecting symmetry. The force of "must" comes from Boundary CFT, the theory of all self-consistent boundary conditions on any CFT. These author's argue that there is an equivalence between dynamical perturbations that drive the edge into a massive phase and non-free boundary conditions. To fully explore the implications for the Spin-MR constructions is beyond the scope of this thesis, though Boundary FT is used as a tool for fixed-point calculations in Chapter 5. Nonetheless, observe that the only boundary conditions on the critical Ising model allowed by Boundary CFT are the two symmetry breaking ferromagnetic product states and the free boundary [7].

For completeness, I mention another recently proposed test of SPT order. Imposing twisted periodic boundary conditions is shown in the specific examples considered by [23] to yield a numerical test of SPT order that is especially suited to tensor-network wavefunctions. The twist operator in the lattice description of the Ising Spin-MR states is the tensor product, at the auxiliary level, of local Pauli X. I leave for future work the task of carrying through the numerical calculation described in [23].

Entanglement spectra provide a further signature of SPT order, and are the focus of the remainder of this thesis. Unlike the strange-correlator test, calculating the entanglement spectrum of a Spin-MR state is non-trivial. It is the purpose of the next two chapters to develop an algorithm for performing the calculation.

3 Tensor networks and bulk-boundary maps

The purpose of this chapter is to make the mapping from bulk to boundary pictures precise, as a preliminary to the algorithm for computing the entanglement spectra of Spin-MR states presented in chapter 4. I show in this chapter, given any Spin MR state $|\Psi\rangle$ specified by an expression of the form in Eq. (1), how to construct:

1. a state $|B)$ in the boundary picture; and,
2. a mapping $\mathcal{M}$ from bulk to boundary observables;

such that, for every local bulk observable $\mathcal{O}_{(a,j)}$ (the indices a, j locating the observable on a two-dimensional lattice), the following holds:

$$\frac{\langle\Psi|\mathcal{O}_{(a,j)}\mathcal{O}_{(a,k)}|\Psi\rangle}{\langle\Psi|\Psi\rangle} = (B|\mathcal{M}_{\mathcal{O}}(j)\mathcal{M}_{\mathcal{O}}(k)|B). \tag{26}$$

Equation (26) and its n-point generalization make good the claim made in the introduction that there is a holographic correspondence between bulk and boundary pictures. Figure 3 presents a graphical outline of the calculations in this chapter that lead to Eq. (26).

The bulk-boundary map is motivated by the goal of approximating the manybody wavefunction by the vacuum of a continuum field theory, a standard approximation strategy in many-body physics. The approximation is taken in the dilute limit, letting the lattice spacing and the number of particles per lattice-spacing-squared both vanish. The continuum theory has a finite correlation length and thus there exists a second, large-system-size limit that is taken in the next chapter. In this IR limit, the approximate description retains only long-range features. To take both these limits together — dilute and IR — is to assume that the particle density is dilute on the scale of the correlation length but dense on the scale of the system size. In the next chapter, I show that the coefficients of the IR limiting state, when rearranged as a matrix, give the square root of the reduced density matrix for the Spin-MR state on a bipartition.

The continuum description presented in this chapter provides an analytically tractable point of departure for tensor-network-based numerical studies beyond the dilute, IR limit. Tensor networks parameterize the search space for the variational methods that are the work-horses of condensed matter numerics. In that context, how to make the most efficient use of computational resources in performing calculations is a challenging and practically important question. A rule of thumb is to start at the boundary of the network and sweep through the bulk (further elaborated in [31]). The intermediate steps in the sweep can be interpreted as time-evolution of the starting boundary. What is special about Spin-MR states, contrasted with general tensor networks (compare [12]), is that the boundary-evolution operator has a closed form expression in the dilute limit (assuming a closed form for the CFT action), which this chapter derives for general Spin-MR states. In brief, the

boundary evolution is given by the CFT Hamiltonian perturbed by the local term $\phi^* \otimes \phi$, where ϕ is the CFT field in Eq. (1), and ϕ^* acts on a second copy of the CFT Hilbert space, this second copy corresponding to the physical bra of the Spin-MR state. The small parameter in the perturbative expansion is particle fugacity.

There is a deep literature on tensor networks as tools for studying condensed matter physics. The goal of this chapter is to introduce only so much of this technology as is necessary to perform the calculations in Chapters 4 and 5. For a more general review, see [5].

3.1 Definitions

A tensor network decomposition of a wavefunction $|\Psi\rangle \in \mathcal{H}$ comprises a state in some extraneous vector space $|B) \in \mathcal{V}$ together with a linear operator $T : \mathcal{V} \to \mathcal{H}$ such that,

$$|\Psi\rangle = T|B). \tag{27}$$

The state $|B)$ and operator T each factorize as pure tensor products and the physical content of the decomposition consists in associating factor spaces of $\mathcal{V}$ and $\mathcal{H}$ with the local degrees of freedom of the system under study. If the local degrees of freedom described by $|\Psi\rangle$ are non-trivially entangled, then the factorization of $\mathcal{V}$ that factors T is *not* the factorization that factors $|B)$, which is the essential feature that makes tensor network decomposition useful. Namely, that an object that *cannot* be locally factored, $|\Psi\rangle$, is described as the composition of two objects that *can* be locally factored, $|B)$ and T. The two factorizations of $\mathcal{V}$ are interpreted in the following way: one is identified with the vertices and the other the edges of a graph. For example, consider $\mathcal{V} \equiv V^{\otimes n}$,

$$\mathcal{V} = \ldots \otimes (V] \otimes [V) \otimes (V] \otimes [V) \otimes (V] \otimes \ldots \tag{28}$$

Associating factors enclosed in $[\ldots]$ with vertices and $(\ldots)$ with edges gives the graph shown in Fig. 4.

The number of factors associated with an edge is always two. The number of factors associated with a vertex is $v+d$ where v is the valence (number of edges) of the vertex and d is the number of boundary degrees of freedom associated with the vertex. The introduction of the notion of boundary degrees of freedom presupposes a chosen interpretation of the graph as a discrete approximation of space-time: for example, in Fig. 4(b) we have set $d = 1$ for the valence-one vertices and $d = 0$ for the valence-two vertices, appropriate if we are interpreting the graph as a discrete approximation of a line-segment.

The same factorization of T also yields a notion of locality for $\mathcal{H} \ni |\psi\rangle$ and hence of local observables. Let $\mathcal{O}$ be a finite product of such observables: the object $T^\dagger \mathcal{O} T$ then factorizes as a linear functional over $\mathcal{V}^* \otimes \mathcal{V}$. The graphical interpretation of the pairing of factors V and V^* is as edges joining the union of two copies of the graph corresponding to $|\psi\rangle$.

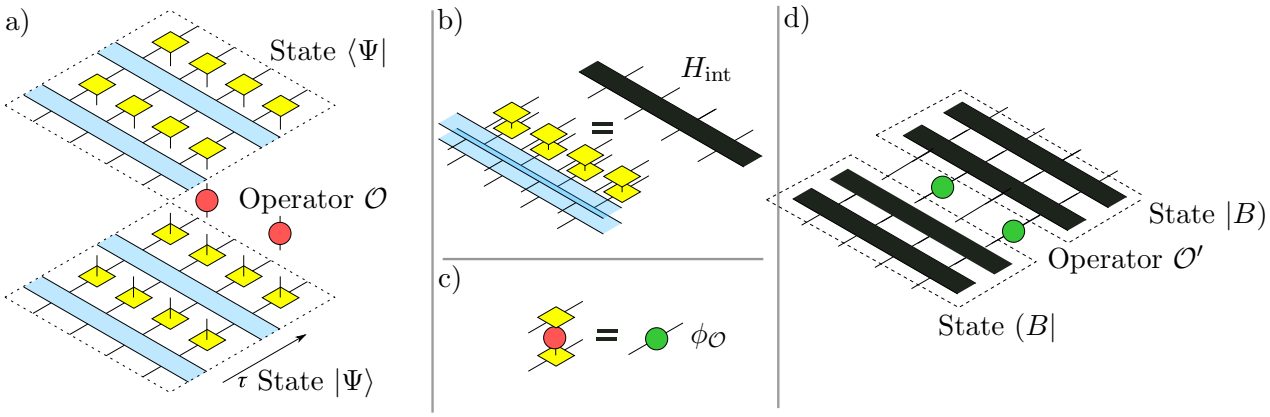

Figure 3: Graphical representation of the calculations in this chapter: the physical Hilbert space comprises vertical legs and the auxiliary CFT Hilbert space comprises horizontal legs; the dashed lines signify the elision of the remainder of the network; **subfigure (a)** shows an expectation value expressed as the contraction of a tensor network: reading the subfigure from bottom to top, the uncontracted vertical legs represent the tensor factors of the state vector; yellow boxes are field insertion tensors $A^i{}_{jk} \equiv \mathbb{I} \otimes |0\rangle + \mu\phi \otimes |1\rangle$ where ϕ is the local field in the auxiliary CFT, as it appears in Eq. (1), and μ is a fugacity that suppresses total particle number; blue rectangles are the (imaginary) time evolution operator that evolves the CFT Hilbert space by one time-step; red circles are local physical operators the dual state appears above; **subfigure (b)** shows how groups of tensors from bra and ket in subfigure (a) contract to form operators on the product of two copies of the auxiliary Hilbert space; the operator shown acts to evolve the boundary according to the interacting Hamiltonian defined in Eq. (50), namely, the CFT Hamiltonian perturbed by the term $\phi^* \otimes \phi$; **subfigure (c)** shows how to express the mapping $\mathcal{M}$ from bulk observable $\mathcal{O}$ to boundary observable $\mathcal{M}_{\mathcal{O}}$ by contracting $\mathcal{O}$ with the field insertion tensors to give local observables in the boundary theory; the subfigure shows that the Spin-MR structure guarantees that local observables translate to local observables in the bulk-boundary dictionary; **subfigure (d)** shows the expectation value in the boundary theory equivalent to subfigure (a); the rows of imaginary-time evolution operators are effectively approximated by the ground state $|B)$ of the Hamiltonian in Eq. (50). The remainder of the chapter works through the algebra from subfigure (a) to (d) for general Spin-MR states in the dilute limit $\mu \sim 0$.

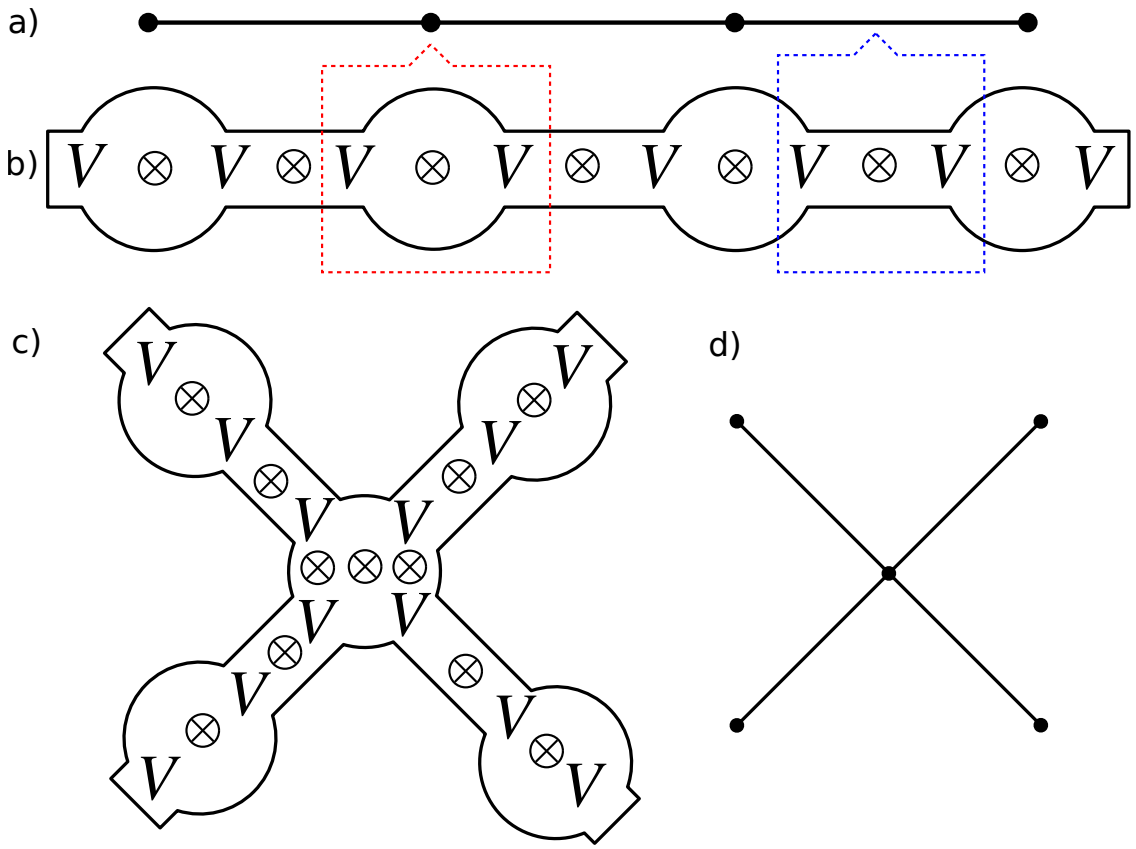

Figure 4: (a)-(b) a tensor network maps the vertices and edges of a graph to factors V of a tensor product space $V^{\otimes n}$; each edge maps to two factors and each vertex to a number of factors at least equal to the vertex valence, any additional factors accounting for boundary conditions; (c)-(d) the factorization of the central valence-four vertex involves an ambiguity that is unimportant because of the associative property of the tensor product. That is, we can take the X shape as the product of two chains) and (or as the product of two chains $\cup$ and $\cap$, and the associative property guarantees that these two products are identical.

Numerically efficient contractions of the tensor network begin from the boundary of the graph. Algebraically, this technique takes an element of the factor space $x^{ij} \in V^* \otimes V$ and its dual $y_{ij} \in V^* \otimes V$ and treats the remainder of the network as a spatial evolution operator $U(\mathcal{O})^{ij}{}_{k\ell}$. The expectation value $y_{k\ell} U(\mathcal{O})^{k\ell}{}_{ij} x^{ij}$ is analogous to the overlap of initial and final states subject to evolution under an external force f, with $\mathcal{O}$ the analog of the forcing term. The construction of Spin MR states supplies a field-theoretic interpretation of $U(\mathcal{O})$ as Euclidean time evolution of a perturbed CFT. A dictionary that translates observables in this field theory to observables acting on $\mathcal{H} \ni |\psi\rangle$ simplifies numerical and analytical calculations in the latter setting.

3.2 Generating functionals for spin lattice observables

This subsection defines a precise equivalent on the lattice to the definition of Spin-MR states given by Eq. (1). The exponential on the right-hand-side of Eq. (1) is a generating functional for (products of) local observables, and so the logical first step towards the goal of this subsection is to define the lattice equivalent of a generating functional. Suppose the space $\mathcal{H}$ to be a tensor product of N copies of a local Hilbert space $\mathcal{H} = \bigotimes_{i=1}^{N} \mathcal{H}_{(i)}$, all $\mathcal{H}_{(i)}$ isomorphic. Let the isomorphic image of any operator $A_{(1)} \in \mathrm{Hom}\left(\mathcal{H}_{(1)}\right)$ in $\mathrm{Hom}\left(\mathcal{H}_{(k)}^{\mathrm{Phys}}\right)$ be denoted $A_{(k)}$; the use of round brackets is intended to clarify that the subscript does not index components. Treat $\mathbb{C}^N$ as the set of functions from the local labels $1 \leq N$ to $\mathbb{C}$. Let $Q_{(1)} \in \mathrm{Hom}\left(\mathcal{H}_{(1)}^{\mathrm{Phys}}\right)$ be a local observable and $f \in \mathbb{R}^N$. A generating functional for a quantum field is a functional whose power series expansion yields all possible correlation functions of the field. Thus, a generating functional for $Q_{(k)}$ is,

$$\mathcal{M}(f, Q) = \bigotimes_{i=1}^{N} \left(\mathbb{I}_{(i)} + \hat{e}_i(f) Q_{(i)}\right), \tag{29}$$

where e_i, $\hat{e}_k$ are basis functions (functionals) satisfying $\hat{e}_i(e_k) = \delta_{ik}$. To check the generating property,

$$\left.\frac{\partial}{\partial e_k}\right|_{f=0} \mathcal{M}(f, Q) = \sum_{i=1}^{N} \delta_{ik} Q_{(k)} \bigotimes_{j \neq k} (\mathbb{I}_j + \hat{e}_j(f) Q_{(j)}) = Q_{(k)} \otimes \mathbb{I}^{\otimes_{i \neq k}^{N}}. \tag{30}$$

From here on, for any local operator $A_{(i)}$, let $A_{(i)}^{\otimes \mathbb{I}}$ abbreviate $A_{(i)} \otimes \mathbb{I}^{\otimes_{p \neq i}^{n}}$. The right-hand-side of Eq. (30) is like the exponentiation of the local observable over the tensor product: indeed, a second generating functional is defined by the ordinary operator exponential as,

$$\tilde{\mathcal{M}}(f, Q) := \exp\left(\sum_{i=0}^{N} \hat{e}_i(f) Q_{(i)}^{\otimes \mathbb{I}}\right). \tag{31}$$

If $Q^2 = 0$ then $\mathcal{M}(f,Q) = \tilde{\mathcal{M}}(f,Q)$, that is, the two generating functionals only differ in terms involving higher powers of the local operator. The notation $**$ is introduced to express this identification, namely, $*\tilde{\mathcal{M}}* = \mathcal{M}$.

The exponent in Eq. (1) is an integral over (imaginary) time and thus, to define its lattice equivalent, we must introduce a notion of time into our lattice of N sites. For the sake of concreteness, suppose our space-time $\mathcal{M}$ is a rectangular array of $n \times m = N$ events equipped with a homogeneous euclidean metric. Columns are the loci of equal space and rows equal imaginary time. Let an auxiliary Hilbert space Aux be a tensor product of n copies of a local Hilbert space $\text{Aux} = \bigotimes_{i=1}^{n} \text{Aux}_{(i)}$. This Aux is the space of quantum states on an equal time slice of $\mathcal{M}$. Suppose a Hamiltonian H_0 defined on Aux generating the one parameter family of unitary transformations $U(t) = \exp(-itH_0)$. Analytically continue these operators to functions of pure imaginary arguments. Let Δ be some small real number (time step) and for any local operator $Q_{(j)}$ understand $Q[j,k]$ to denote,

$$Q[j,k] := U(-ik\Delta) Q_{(j)}^{\otimes \mathbb{I}} U(ik\Delta). \tag{32}$$

A generating functional for local time dependent observables is then

$$\mathcal{M}(f,V) := T\left\{ * \exp\left(\sum_{j=0}^{n} \sum_{i=0}^{n} \hat{e}_{i,j}(f) Q[i,j] \right) * \right\} \tag{33}$$

with $T\{\cdot\}$ the time-ordering operator having the usual meaning that products of $Q[i,j]$ in the power-series of the exponential are imaginary-time ordered.

The function $\mathcal{M}(f,V)$ defined in Eq. (33) is not linear in f but a linear equivalent can be defined on a suitable Hilbert space. Consider all functions in ${Z_2}^N$ and treat each function elements in this set as a basis vector in a 2^N complex dimensional vector space. Let $\mathbf{e}_0$ be a local zero and $\mathbf{e}_1$ a local one so that the basis vector $\mathbf{f} \in \mathbb{C}^{2^N}$ is the N fold tensor product $\bigotimes_{i=0}^{n} \bigotimes_{j=0}^{n} \mathbf{e}_{f(i,j)}[i,j]$, the square brackets indexing the sites. Introduce a local annihilation operator $a[i,j]$ on this space that decrements basis functions in the obvious way. Let $\mathbf{0}$ be the all zeros basis element and denote duals by hats. A linear generating functional is,

$$L(\mathbf{s},Q) = \hat{\mathbf{0}} T\left\{ * \exp\left(\sum_{j=0}^{n} \sum_{i=0}^{n} a[i,j] \otimes Q[i,j] \right) * \right\} \mathbf{s}, \quad \mathbf{s} \in \mathbb{C}^{2^N}. \tag{34}$$

The lattice equivalent to the definition of Spin-MR-States in Eq. (1) is therefore as follows. Suppose $\mathcal{H}_{\text{Phys}} \cong \mathbb{C}^{2^N}$. The expectation value of (the dual of) L taken against any state

in Aux, and in particular, $\lim_{\beta\to\infty} U(-i\beta)/\mathrm{Tr}[U(-i\beta)]$, defines a state $|\Psi\rangle \in \mathcal{H}$,

$$|\Psi\rangle := \lim_{\beta\to\infty} \frac{1}{\mathrm{Tr}\left[U(-i\beta)\right]} \mathrm{Tr}\left[U(-i\beta)T\left\{*\exp\left(\sum_{j=0}^{n}\sum_{i=0}^{n} a^\dagger[i,j]\otimes Q[i,j]\right)*\right\}\right]\mathbf{0}. \quad (35)$$

There are two important caveats attaching to the right-hand-side of Eq. (35). The operator $\lim_{\beta\to\infty} U(-i\beta)/\mathrm{Tr}[U(-i\beta)]$ projects on to the ground state of H_0: the choice of this operator is not essential to our construction and can be replaced with other asymptotic states that encode initial and final conditions. The second, related warning is that we need also to impose spatial boundary conditions.

3.3 Spin-Moore-Read States approximated as Projected Entangled Pair States

The $|\Psi\rangle$ defined in Eq. (35) is equivalent to a translation-invariant, two dimensional tensor network of a standard form: a *Projected Entangled Pair State* (*PEPS*) [45], up to boundary tensors. To see the equivalence, define a three index tensor,

$$A^i_{j,k} \equiv \mathbb{I}\otimes \mathbf{e}_0 + Q\otimes \mathbf{e}_1, \quad (36)$$

where $\mathbb{I}, Q$ are matrices determining the lower indices and $\mathbf{e}_{0,1}$ are basis vectors for the upper, physical index. Let $A^{\mathbf{i}}$ denote the n fold tensor power of A, the physical indices labeled by a column vector $\mathbf{i}$ and define an $n\times n$ dimensional tensor $\Psi^{[\mathbf{i}]}$ with the index values represented by a row vector $[\mathbf{i}]$ of column vectors as follows,

$$\Psi^{[\mathbf{i}]} = \mathrm{Tr}\left[U(-i\infty)A^{\mathbf{i}_0}U(-i\Delta)A^{\mathbf{i}_1}U(-i\Delta)\ldots A^{\mathbf{i}_n}\right]/\mathrm{Tr}[U(-i\infty)]. \quad (37)$$

The vectorized $\Psi^{[\mathbf{i}]}$ is $|\Psi\rangle$. Because tensor network decompositions are not unique, choosing a network representation of $|\Psi\rangle$ does not fix the network representation of $\langle\Psi|$ for the purpose of computing expectation values. Our choice for $\langle\Psi|$ is to fix a basis and take component-wise complex conjugates of the constituent tensors of our representation of $|\Psi\rangle$ as follows,

$$\Psi^{[\mathbf{i}]*} = \sum_{\alpha\beta\ldots\omega} U(-i\infty)^*_{\alpha\beta}A^{\mathbf{i}_0*}_{\beta\gamma}U(-i\Delta)^*_{\gamma\delta}A^{\mathbf{i}_1*}_{\delta\epsilon}U(-i\Delta)^*_{\epsilon\kappa}\ldots A^{\mathbf{i}_n*}_{\omega\alpha}/\mathrm{Tr}[U(-i\infty). \quad (38)$$

There is a basis free description of this construction of $\langle\Psi|$ in terms of an anti-unitary operator $(*)$ acting on the auxiliary Hilbert space. Let $|i\rangle \in$ Aux and let $U_{(r)}$ be the change to our preferred basis. Then $\left|i^{(*)}\right\rangle = U^{-1}_{(r)}\left[U_{(r)}|i\rangle\right]^*$. Likewise, the action on operators is defined $A^{(*)} = U^{-1}_{(r)}\left[U_{(r)}AU^{-1}_{(r)}\right]^* U_{(r)}$.

The adjoint also gives a basis free description of $\langle\Psi|$,

$$\Psi^{[\mathbf{i}]*} = \mathrm{Tr}\left[\left(U(-i\infty)A^{\mathbf{i}_0}U(-i\Delta)A^{\mathbf{i}_1}U(-i\Delta)\dots A^{\mathbf{i}_n}\right)^\dagger\right]/\mathrm{Tr}[U(-i\infty)]. \tag{39}$$

However, pulling through † reverses the ordering of physical indices in the time direction, whereas we want a picture in which time flows in the same direction as between bra and ket. In this way, we are able to provide an equivalent description of the contraction $\sum_{[\mathbf{i}],[\mathbf{j}]}\Psi^{[\mathbf{i}]*}\mathcal{O}^{[\mathbf{i}],[\mathbf{j}]}\Psi^{[\mathbf{j}]}$ for some physical observable $\mathcal{O}$ as the expectation value of Heisenberg operators on the expanded auxiliary Hilbert space $\mathrm{Aux}\otimes\mathrm{Aux}^{(*)}$.

The network on the right-hand-side of Eq. (37) is not yet a PEPSs. By iterative singular value decomposition, the time-step operator $U(-i\Delta)$ can be put into the form of a translation invariant (on periodic boundary conditions) matrix product operator $M_{\alpha,\beta,i,k}$, as shown in [42] and [17], where the Greek indices are spatial and the Latin temporal. The tensors in the MPO decomposition do not depend on the system size. Then the PEPS tensor $P^i{}_{\alpha\beta jk}$ is,

$$P^i_{\alpha,\beta,j,k} = \sum_\ell M_{\alpha,\beta,j,\ell}A^i_{\ell,k}. \tag{40}$$

This significance of the tensor $P^i{}_{\alpha\beta jk}$ is that its tensor powers define the operator T in Eq. (27). Together with a graph whose vertices all have valence four (corresponding to the four lower tensor indices), $P^i{}_{\alpha\beta jk}$ maps the set of boundary conditions on the graph to a set of states in $\mathcal{H}$, an example of which is shown in Fig. 5.

The PEPS description is not complete without specifying initial and final conditions in imaginary time. The partially contracted network, with all virtual indices contracted save the indices at the initial and final time, is a rank three tensor $\Theta^i{}_{\alpha\beta}$ with the first index ranging over the physical Hilbert space and the second and third indices ranging over the initial and final auxiliary Hilbert spaces. The choice of initial and final states implied by the Spin-MR construction is the ground state of the quantum critical 1+1 D transverse field Ising model Ω^α, so that the Spin MR-State is $\Theta^i{}_{\alpha\beta}\Omega^\alpha\Omega^{*\beta}$. But, unlike the PEPS tensor $P^i{}_{\alpha\beta jk}$, a tensor network decomposition of Ω^α must depend on the total system size. Because the correlation length of Ω^α is infinite, the Hilbert space dimension of the auxiliary spatial indices — the "bond dimension" — at initial and final times must grow logarithmically in the system's length [47]. The PEPS literature typically only considers finitely correlated boundaries, since constant scaling of bond-dimension is an assumption of the usual numerical calculations performed with PEPS. Nonetheless, observables deep in the bulk of $|\Psi\rangle$ do not depend on the detailed features of Ω^i, only its symmetries. Expectations of bulk observables depend instead on the fixed point of a transfer matrix constructed out of $P^i{}_{\alpha\beta jk}$ alone. This fixed point calculation, performed in Chapter 4, is the typical approach in PEPS numerics.

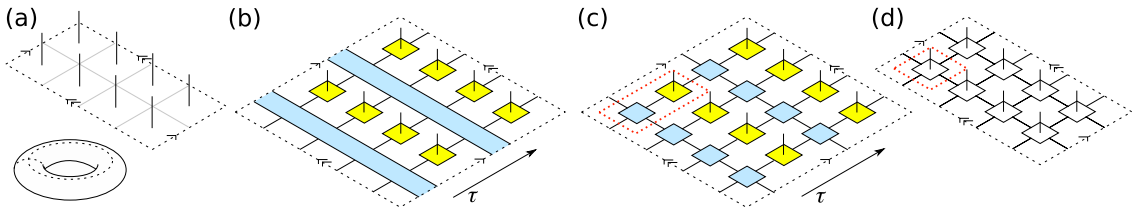

Figure 5: The decomposition of a Spin-MR state on a torus into a *Projected Entangled Pair State* (PEPS); (a) the torus unfolds into a rectangular array of local degrees of freedom subject to periodic boundary conditions; the vertical legs are the free indices of these degrees of freedom; (b) identifying one axis of the array with time, the << boundary of the rectangle is the auxiliary space Aux; the blue rectangles are imaginary-time-step-evolution operators acting on Aux; the yellow squares are the field insertion tensors defined in Eq. (36); (c) the time-step-evolution operators decompose as tensors along the spatial dimension into space-time evolution operators; (d) by contracting a field insertion operator with a space-time evolution operator, an array of identical PEPS tensors, shown as white squares, is obtained; now reading the flow from (d) to (a), starting with a PEPS tensor we obtain an entangled state on a torus.

Therefore, $|\Psi\rangle$ admits a PEPS description for all and only local observables deep in the bulk. The meaning of "deep" is given by the the bulk-correlation length, and is not necessarily related to distance from any bulk-picture boundary. For example, in the toroidal geometry shown in Fig. 5, so long as the circumference of the torus in the time direction is many multiples of the PEPS tensor correlation length, then all two-point correlators are "deep" in the bulk. On the other hand, Spin-MR state expectations of non-local observables that probe total system size cannot be computed in the PEPS formalism. The clearest example of the difficulties posed by a non-local observable is the strange-correlator introduced in Chapter 2, which projects $|\Psi\rangle$ onto the sector of the physical Hilbert space with total particle number equaling two. Looking again at Fig. 5, the amplitude of the zero-particle component of the network is the euclidean path integral of the 1+1 D quantum transverse field Ising model at non-zero temperature (up to a factor that normalizes the wavefunction). The temperature is non-zero because the radius of the time circumference is finite, and a non-zero temperature implies the partition function is in a disordered phase. Thus, the strange correlators of the network in Fig. 5 must decay exponentially, with algebraic decay only recovered in the infinite size (zero-temperature) limit. But since the strange correlators of Spin-MR states with the zero-particle state are algebraic by construction, it follows that the finite-sized network shown in Fig. 5 is not strictly a Spin-MR State. The fact that the PEPs tensor does not convey the non-local properties of the Spin-MR state is another hint that Spin-MR States *can have* interesting non-local properties.

3.4 Bulk-boundary dictionary

This subsection carries out the calculation shown in Fig. 3(c): given a bulk-picture observable $\mathcal{O}$, it shows how to compute the boundary-picture observable $\mathcal{M}_{\mathcal{O}}$. The mapping in hand, the subsection computes the boundary-picture Hamiltonian shown in Fig. 3(b).

Recall that each physical spin index is attached to a tensor $A^i_{j,k} \equiv \mathbb{I} \otimes \mathbf{e}_0 + Q \otimes \mathbf{e}_1$, where the bold faced vectors are basis elements for the physical index i. The action of the local physical observable on an isolated physical leg goes like,

$$(\mathbb{I} \otimes \mathcal{O})(\mathbb{I} \otimes \mathbf{e}_0 + Q \otimes \mathbf{e}_1) = \mathbb{I} \otimes \mathcal{O}\mathbf{e}_0 + Q \otimes \mathcal{O}\mathbf{e}_1. \tag{41}$$

The generating functional $\mathcal{M}(\mathcal{J}, \mathcal{O})$ defined in Eq. (29) thus contracts locally as,

$$\begin{aligned}
&\sum_{i=0}^{1} (\mathbb{I}\ (\hat{\mathbf{e}}_i \mathbf{e}_0) + Q^{(*)}\ (\hat{\mathbf{e}}_i \mathbf{e}_1)) \otimes (\mathbb{I}\ [\hat{\mathbf{e}}_i (\mathbb{I} + \mathcal{J}\mathcal{O}) \mathbf{e}_0] + Q\ [\hat{\mathbf{e}}_i (\mathbb{I} + \mathcal{J}\mathcal{O}) \mathbf{e}_1]) \\
=&\mathbb{I} \otimes \mathbb{I} + Q^{(*)} \otimes Q + \mathcal{J} \Big(\mathcal{O}_{00}\ \mathbb{I} \otimes \mathbb{I} + \mathfrak{Re}[\mathcal{O}_{01}]\ (\mathbb{I} \otimes Q + Q^{(*)} \otimes \mathbb{I}) \\
&+ i \mathfrak{Im}[\mathcal{O}_{01}]\ (\mathbb{I} \otimes Q - Q^{(*)} \otimes \mathbb{I}) + \mathcal{O}_{11}\ Q^{(*)} \otimes Q \Big).
\end{aligned} \tag{42}$$

Let (x, t) be space-time coordinates of the auxiliary system. We imagine duplicating the lattice on which $|\Psi\rangle$ is defined and layering the copies so that cloned sites align in a vanishingly thin y dimension. We fix an orientation so that the normal to the top layer points in the positive y direction and the normal to the bottom the negative. Then, relative to the global x, t coordinates, we may describe the top layer as right-handed and the bottom layer left-handed. We treat pairs of cloned sites as single super-sites with expanded local Hilbert space $\mathrm{Aux} \otimes \mathrm{Aux}^{(*)}$. Define an anti-unitary parity transformation on the operators of this super-local space as,

$$P[A \otimes B] = B^{(*)} \otimes A^{(*)}. \tag{43}$$

The operator P is obviously involutive and has eigenvalues ± 1 corresponding to parity even or odd operators. Define the parity even, free super-local Hamiltonian,

$$H_{\text{free}} = \mathbb{I} \otimes H_0 + H_0^{(*)} \otimes \mathbb{I}. \tag{44}$$

Because the terms on the right hand side commute,

$$\exp(-\Delta H_{\text{free}}) = U(-i\Delta)^{(*)} \otimes U(-i\Delta). \tag{45}$$

Equation (42) reveals the bulk-boundary dictionary. Equation (42) shows that every local physical observable $\mathcal{O}$ pulls into the doubled auxiliary theory as a linear combination $\mathcal{M}_{\mathcal{O}}$ of:

1. the identity;
2. the mass density $\rho := Q^{(*)} \otimes Q$;
3. the parity even field $p^+ := \mathbb{I} \otimes Q + Q^{(*)} \otimes \mathbb{I}$; and,
4. the parity odd field $p^- := i\ (\mathbb{I} \otimes Q - Q^{(*)} \otimes \mathbb{I})$.

It is helpful to make the dimensions of ρ more explicit by redefining $\rho^{\text{new}} := \rho^{\text{old}}/\Delta\mu$, μ having dimensions of energy and interpreted as a chemical potential, arbitrary up to redefining Q by scalar multiplication.

From Eq. (42), the definition of $|\Psi\rangle$ in Eq. (37) and the expression for $\langle\Psi|$ in Eq. (38), it follows immediately that,

$$\langle\Psi|\mathcal{M}(\mathcal{J},\mathcal{O})|\Psi\rangle = \lim_{\beta\to\infty} \frac{\text{Tr}\left[\exp(-\beta H_{\text{free}}) \prod_{k=1}^{m} \left(\exp\left(-\Delta H_{\text{free}}\right) \bigotimes_{j=1}^{n} \left(\mathbb{I} + \left[\mu\rho_{(j)} + \hat{e}_{j,k}(\mathcal{J})\mathcal{M}_{\mathcal{O}}\right]\right)\right)\right]}{\text{Tr}\left[\exp(-\beta H_{\text{free}})\right]}. \quad (46)$$

Now allow the number of time slices m to vary. We are going to take the limit as the time steps vanish in size. A technical issue in taking the limit is making sense of $\hat{e}_{j,k}(\mathcal{J})$. Let us use as the second index the rational number $k/m \in (0,1)$ and only consider $\mathcal{J}$ supported at $k/m = 1$. The claim we make is that,

$$\lim_{m\in\mathbb{N}\to\infty} \prod_{k=1}^{m} \left(\exp\left(-\frac{1}{m}H_{\text{free}}\right) \bigotimes_{j=1}^{n} \left(\mathbb{I} + \frac{1}{m}\left[\mu\rho_{(j)} + \hat{e}_{j,k/m}(\mathcal{J})\mathcal{M}_{\mathcal{O}}\right]\right)\right)$$
$$= \exp\left(-H_{\text{free}} + \sum_{j=1}^{n} \mu\rho_{(j)} + \hat{e}_{j,1}(\mathcal{J})\mathcal{M}_{\mathcal{O}}\right). \quad (47)$$

The proof is almost exactly as for the more familiar Totter formula. Using the abbreviation $A_{(i)} := \mu\rho_{(i)} + \hat{e}_{i,1}(\mathcal{J})\mathcal{M}_{\mathcal{O}}$ and applying the Baker-Campbell-Hausdorff formula, it follows that,

$$\lim_{m\in\mathbb{N}\to\infty} \left(\exp\left(-\frac{1}{m}H_{\text{free}}\right) \bigotimes_{j=1}^{n} \left(\mathbb{I} + \frac{1}{m}A_{(i)}\right)\right)^{m}$$
$$= \lim_{m\in\mathbb{N}\to\infty} \exp\left(m \ln\left[\exp\left(-\frac{1}{m}H_{\text{free}}\right) \exp\left(\sum_{i=1}^{n}\sum_{q=1}^{\infty} \frac{1}{qm^q}\left(A_{(i)}^{q}\right)^{\otimes\mathbb{I}}\right)\right]\right)$$
$$= \lim_{m\in\mathbb{N}\to\infty} \exp\left(-H_{\text{free}} + \sum_{i=1}^{n} A_{(i)}^{\otimes\mathbb{I}} + \mathcal{O}\left(m^{-1}\right)\right). \quad (48)$$

The elided terms are a power series in m^{-1} with operator valued coefficients given by nested commutators of A_i and H_{free} summed with higher local powers of $A_{(i)}$. The order m^{-1} terms indicate that the rate of convergence is governed by the chemical potential and the characteristic time τ of the free evolution of ρ:

$$\mathcal{O}(m^{-1}) = \frac{1}{m}\sum_{i=1}^{n}[H_{\text{free}}, A_i] + \frac{1}{2m}\sum_{i=1}^{n}\left(A_{(i)}^2\right)^{\otimes \mathbb{I}} + \mathcal{O}(m^{-2}) \sim \frac{n\mu}{m\tau} + \frac{n\mu^2}{2m} + \mathcal{O}(m^{-2}), \quad (49)$$

so that an estimate of the multiplicative error is $\left(1 + \frac{n\mu}{m\tau} + \frac{n\mu^2}{2m}\right)$.

The next step is to define an interacting Hamiltonian on $\mathcal{H}_{\text{Aux}}^{(*)} \otimes \mathcal{H}_{\text{Aux}}$,

$$H_{\text{int}} := H_{\text{free}} - \sum_{i=1}^{n} \mu \rho_{(j)}^{\otimes \mathbb{I}}, \quad (50)$$

allowing a rewriting of Eq.(46) as,

$$\langle \Psi | \mathcal{M}(\mathcal{J}, \mathcal{O}) | \Psi \rangle = \lim_{\beta\to\infty, \gamma\to\infty} \frac{\text{Tr}\left[\exp\left(-\gamma H_{\text{free}}\right) \exp\left(-\beta H_{\text{int}} + \sum_j^n \hat{e}_{j,1}(\mathcal{J}) \mathcal{M}_{\mathcal{O}}\right)\right]}{\text{Tr}\left[\exp(-\gamma H_{\text{free}} - \beta H_{\text{int}})\right]}. \quad (51)$$

The final step is to define also a boundary state $|B_{\beta,\ |\text{i.c.})}) \in \text{Aux}^{(*)} \otimes \text{Aux}$, depending on a parameter β that measures a total duration of imaginary-time and on initial conditions $|\text{i.c}^{(*)})|\text{i.c.})$,

$$|B_{\beta,\ |\text{i.c.})}) = \exp\left(-\beta H_{\text{int}}\right) |\text{i.c.}^{(*)})|\text{i.c.}) / \sqrt{(\text{i.c.}^{(*)}|(\text{i.c.}| \exp\left(-\beta H_{\text{int}}\right) |\text{i.c.}^{(*)})|\text{i.c.})}, \quad (52)$$

For the state defined by Eqs. (35,37), the initial conditions are the ground state of H_0. Let us define $|B) \in \text{Aux}^{(*)}\text{Aux}$ to be the $\beta \to \infty$ limit of $|B_{\beta,\ |\text{i.c.})})$ under these initial conditions,

$$|B)(B| := \lim_{\beta\to\infty} \lim_{\gamma\to\infty} \frac{\exp(-\beta H_{\text{int}}) \exp(-\gamma H_{\text{free}}) \exp(-\beta H_{\text{int}})}{\text{Tr}[\exp(-2\beta H_{\text{int}}) \exp(-\gamma H_{\text{free}})]}. \quad (53)$$

The functional derivative may be taken outside the brackets in an expectation value,

$$\langle \Psi | \mathcal{O}_k | \Psi \rangle = \langle \Psi | \frac{\delta}{\delta e_k}\Big|_{f=0} \mathcal{M}(f, \mathcal{O}) | \Psi \rangle = \frac{\delta}{\delta e_k}\Big|_{f=0} \langle \Psi | \mathcal{M}(f, \mathcal{O}) | \Psi \rangle . \quad (54)$$

By combining Eqs.(51), (53) and (54), and taking repeated functional derivatives, it follows that in the double limit,

$$\lim_{\beta\to\infty} \lim_{\Delta\to 0} \frac{\langle \Psi | \mathcal{O}_{(a,j)} \mathcal{O}_{(a,k)} | \Psi \rangle}{\langle \Psi | \Psi \rangle} = (B | \mathcal{M}_{\mathcal{O}}(j) \mathcal{M}_{\mathcal{O}}(k) | B), \quad (55)$$

as promised at the outset of this chapter. The boundary state $|B)$ summarizes all there is to know about $|\Psi\rangle$ in the continuum, large system size limit, and in the next chapter we present an algorithm that extracts from $|B)$ the entanglement spectrum of $|\Psi\rangle$. The entanglement spectrum provides us with a numerical signature of SPT order.

4 An algorithm to compute bipartite entanglement spectra

4.1 Aim and summary

The aim of this chapter is to propose and verify an algorithm that computes the low-energy part of the bipartite entanglement spectrum of general Spin MR State $|\Psi\rangle$. A degenerate or gapless spectrum (a notion made precise below) is a signature of SPT order. The algorithm is presented in the tensor network formalism introduced in Chapter 3. To summarize the algorithm in four steps:

1. Construct the interacting Hamiltonian H_{int} on $\text{Aux} \otimes \text{Aux}^{(*)}$ (defined in Eq.(50));
2. Find the ground state $|B)$ of H_{int} in an $\text{Aux} \otimes \text{Aux}^{(*)}$ product basis $\{|i)|j)\}$;
3. Construct the matrix B_{ij} from the components of $|B) = \sum_{ij} B_{ij}|i)|j)$;
4. Find the leading eigenvalues λ_0, λ_1 of B^2: the entanglement spectral gap is $\ln(\lambda_0/\lambda_1)$.

By a change of basis, explicitly constructed in this chapter, the matrix B^2 becomes the reduced density matrix of $|\Psi\rangle$ on a real-space bipartition in the infinite system-size limit. The algorithm combines (i) the result in [12], that the physical reduced density matrix of a PEPS is unitarily similar to the square of a "virtual density matrix" on the auxiliary space, with (ii), the construction of the Schmidt basis for MR states presented in [15].

4.2 Motivation

Before proceeding to the technical details of the algorithm, it is worth recalling the physical significance of bipartite entanglement entropy and the entanglement spectrum. Entropy quantifies how much information can be gained from measuring a physical system, given present knowledge of its state. For the purpose of illustrating this information-theoretic perspective on entropy, suppose we have an unbiased coin and we are interested in the question: if we toss the coin now, will the coin land heads? Our knowledge of the state of the system is expressed in the probability distribution:

$$p : \{0, 1\} \to [0, 1] \subset \mathbb{R}; \quad p(0) = 0.5,\ p(1) = 0.5. \tag{56}$$

The *Shannon entropy* of p measured in *bits* is

$$S(p) := \sum_{x \in \{0,1\}} -p(x)\log_2 [p(x)] = 1. \tag{57}$$

In words, Eq. (57) says that measuring the result of the coin toss yields one bit of information, because the measurement answers one yes-or-no question about which we were

entirely ignorant prior to making the measurement. Suppose instead the limiting case of a biased coin:

$$p(0) = 1,\ p(1) = 0 \implies S(p) = 0. \tag{58}$$

According to the definition of $S(p)$ in Eq. (57), the entropy vanishes, meaning that the measurement yields zero bits of information (because the outcome of the coin-toss is a sure-thing). The *von Neumann entropy* of a quantum density matrix ρ is defined more generally,

$$S(\rho) := \mathrm{Tr}\left[-\rho \ln \rho\right]. \tag{59}$$

It follows from Eq. (59) that the von Neumann entropy of a pure quantum state vanishes. Meaning, there is no further information about a system known to be in a quantum pure state that an experimenter can gain from performing a measurement on it (which is consistent with the interpretation that the result of the measurement is non-deterministic).

To make the connection with bipartite entanglement entropy, consider a system divided into two parts: A and B. Without loss of generality, assume that the number of degrees of freedom contained in A is less than or equal to the number in B. Bipartite entanglement entropy quantifies the amount of information about subsystem A to be gained by measuring subsystem B. More precisely, given a pure state of the total system, $|\psi\rangle \in A \otimes B$, and some product-basis expression for $|\psi\rangle$,

$$|\psi\rangle := \sum_{i,j} \psi_{i,j} \left|\xi_i\right\rangle \left|\chi_j\right\rangle, \quad \mathrm{span}\{|\xi_i\rangle\} = A,\ \mathrm{span}\{|\chi_j\rangle\} = B, \tag{60}$$

the reduced density matrix on A of $|\psi\rangle$ is,

$$\rho_{A\backslash B} := \sum_{i,j} \left(\sum_k \psi_{i,k} \psi^*_{j,k} \right) \left|\xi^i\right\rangle \left\langle\xi^j\right|, \tag{61}$$

and the bipartite entanglement entropy of ψ is the von Neumann entropy of this reduced density matrix:

$$S_{A\backslash B}\left(|\psi\rangle\right) := S(\rho_{A\backslash B}) = \mathrm{Tr}\left(\rho_{A\backslash B} \ln \rho_{A\backslash B}\right). \tag{62}$$

Of particular physical interest are the bipartite entanglement entropies of ground states, i.e., low-temperature thermal equilibrium states. The relevant scale against which to compare entanglement entropy is system-size, both the total number of degrees of freedom (in the two-dimensional setting, the surface area) and the number of degrees of freedom along the boundary of the partition (the length of the boundary). At one extreme, if the Hamiltonian does not couple A and B, then the bipartite entanglement entropy of the ground state must vanish independent of area and length (because the two parts do not interact, no information about part A is contained in the degrees of freedom belonging to part B). At the other extreme, a state chosen randomly from the $A \otimes B$ Hilbert space

almost always has entanglement entropy that scales extensively as the number of degrees of freedom in A (recalling that A is smaller than B). The interesting states are therefore those with sub-extensive scaling of entanglement entropy.

A useful mathematical construct for studying Entanglement entropy is the *entanglement Hamiltonian*, defined by:

$$H_E = -\ln(\rho_{A\setminus B}). \tag{63}$$

Defining further a partition function,

$$Z(\beta) := \mathrm{Tr}\left(e^{-H_E\beta}\right), \tag{64}$$

the thermodynamic definition of entropy follows as a mathematical identity:

$$S(\rho_{A\setminus B}) = -\frac{\partial}{\partial\beta}\bigg|_{\beta=1} \log Z. \tag{65}$$

The entanglement Hamiltonian of a topologically trivial wave-function satisfies two conditions. First, the ground state of the entanglement Hamiltonian is unique; second, the next smallest eigenvalue is separated from the ground-state eigenvalue by a gap that is not (or only weakly) suppressed with increasing system size. Let an entanglement Hamiltonian that violates condition (i) be called *degenerate* and one that violates (ii) be called *gapless*. There is a whole set of examples of topologically ordered states with respect to which the entanglement Hamiltonian is a projector, i.e., the excited part of the spectrum is constant, which includes the toric code and string-net states [18], [36]. The paradigmatic example of a topologically ordered wave-function is the Moore-Read FQHE state at five-halves filling [33]: the smallest eigenvalues of the entanglement Hamiltonian of this state correspond to the energy levels of excitations at the physical boundary of the FQHE [30]. An algorithm that, given a wave-function, computes an approximate entanglement spectrum to enough accuracy to determine if the spectrum is degenerate or gapless, can thus provide evidence that the wave-function is in a non-trivial SPT phase [32].

The remaining technical justification of the algorithm in this section assumes spin degrees of freedom that are located on the vertices of a finite-size, square lattice. The motivation for this assumption lies in its making the calculations that verify the algorithm more concrete. Once this planar case is understood, adapting the algorithm to cylindrical and toroidal geometries is uncomplicated. The generalization to *any* surface would follow the method of Topological Quantum Field theory in 1+1 D and break the surface into simpler subsurfaces with boundaries, a natural procedure in the tensor-network formalism [27]. But this generalisation is not pursued here.

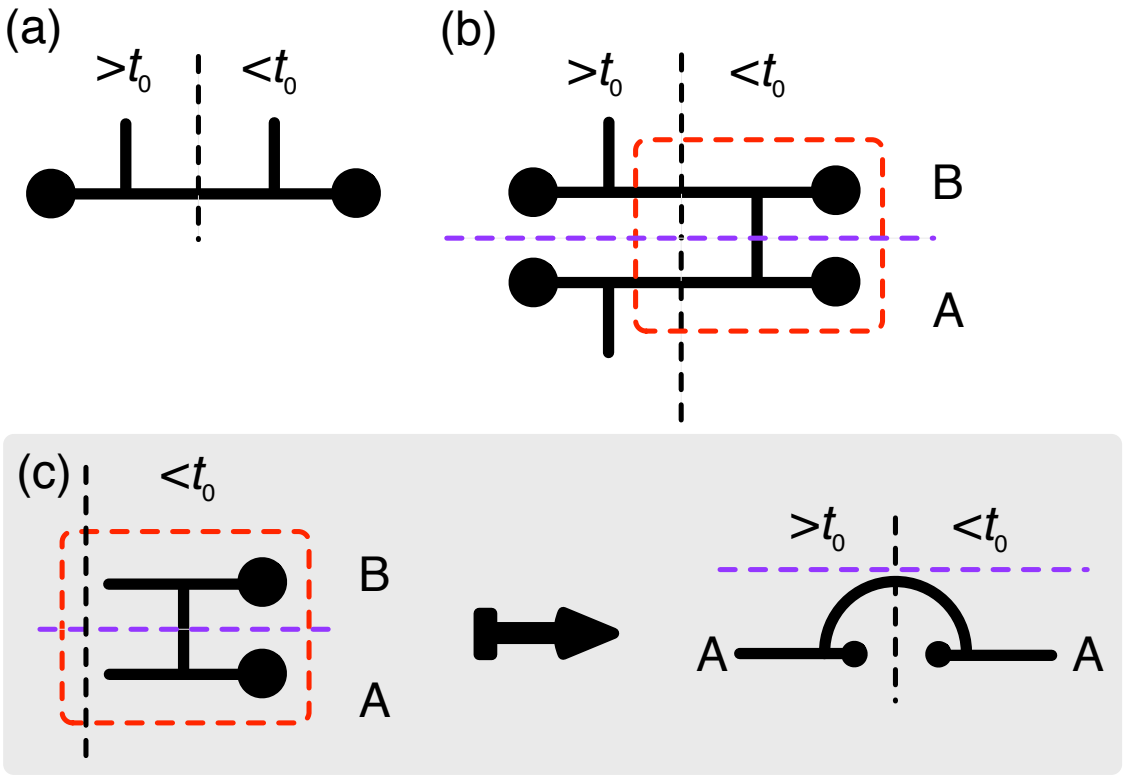

Figure 6: (a) tensor network diagram of state $|\Psi\rangle$ showing the degrees of freedom partitioned about some cut at the imaginary time t_0; (b) the reduced density matrix for the same state for the degrees of freedom in the future of the cut; the vertical space in partitioned into two virtual subsystems A and B as indicated by the blue dashed line; the sub-network in the red box has two free virtual indices as is the ground state of the dynamics described by the Hamiltonian defined in Eq. (50); (c) the virtual ground state transforms into an operator on the A subsystem.

4.3 The algorithm

The output of the algorithm is the entanglement spectrum of the Spin-MR state $|\Psi\rangle$. The state $|\Psi\rangle$ is related to the reduced density matrix $\rho_{A\setminus B}$ by Eq. (61). The $\rho_{A\setminus B}$ eigenbasis may be labeled by pseudo-energies:

$$\rho_{A\setminus B} = \sum_i e^{-\xi_i \beta} |\xi_i\rangle\langle\xi_i|, \tag{66}$$

where β is a dimensional constant set to unity.

To give a synopsis of the detail to follow, figure 6 shows how to compute a reduced density matrix given a tensor-network description of a state. In both sub-figure (b) and on the left-hand-side of sub-figure (c), the virtual state enclosed in the dashed red line is exactly (in the continuum limit) the ground state of the Hamiltonian in Eq. (50).

We seek a component-wise expression for $\rho_{A\setminus B}$. The following choice of orthonormal basis proves to be convenient. Recall that the super auxiliary Hilbert space decomposes as $\mathrm{Aux}^{(*)} \otimes \mathrm{Aux}$. The $(*)$ is an *aide memoire* reminding us which factor corresponds to $\langle\Psi|$. The state $|B)$ defined in Eq. (53) and represented in Fig. 6.(c) decomposes in a tensor product basis as

$$|B) = \sum_{i,j} B_{i,j} |i)|j), \quad |i) \in \mathcal{H}^{(*)}_{\mathrm{Aux}},\ |j) \in \mathcal{H}_{\mathrm{Aux}}, \tag{67}$$

with $\{|i)\}$ an arbitrary basis for $\mathcal{H}_{\mathrm{Aux}}$. The operator on $\mathcal{H}_{\mathrm{Aux}}$,

$$B := \sum_{i,j} B_{i,j} |i)(j^{(*)}|, \tag{68}$$

is Hermitian because the action of the imaginary time evolution operator on $|B)$ is equivalent to the action of a completely positive map on B (the simple demonstration of this fact is left to the end of this section). Hence, B decomposes in some orthonormal basis $\{|B_k)\}$ as,

$$B = \sum_k \lambda_{(B,k)} |B_k)(B_k|, \tag{69}$$

and from here the expression for $|B)$ follows:

$$|B) = \sum_k \lambda_{(B,k)} |B_k)|B_k). \tag{70}$$

The vectors $|B_k)$ then yield orthonormal states $\{|\Psi_{B_k}\rangle\}$ in the bulk-picture Hilbert space

by acting as boundary states in the boundary-picture. First, define,

$$|\Psi_{B_k}\rangle := \lim_{\beta\to\infty} \frac{1}{\sqrt{(B_k^{(*)}|(B_k|\exp\left(-\beta H_{\rm int}\right)|{\rm i.c.}^{(*)})|{\rm i.c.})}}\times$$
$$\lim_{m/\Delta\to\infty}(B_k|:*\exp\left(\sum_{j=0}^{m}\sum_{i=0}^{n}a^\dagger[i,j]\otimes V[i,j]\right)*:|{\rm i.c.})\ \mathbf{0}. \tag{71}$$

Comparing Eq. (71) with the definition of Spin-MR states in Eq. (1), observe that $|\Psi_{B_k}\rangle$ is a Spin-MR state defined by a mixed correlation function in which the in-state differs from the out-state. Each $|\Psi_{B_k}\rangle$ is defined by the same in-state but the out-states vary with the index k. Because the out-states are orthogonal, the $|\Psi_{B_k}\rangle$ are orthonormal, as the next calculation verifies:

$$\langle\Psi_{B_k}|\Psi_{B_\ell}\rangle = \lim_{\beta\to\infty}\Big[(B_k|(B_\ell|\exp\left(-\beta H_{\rm int}\right)|{\rm i.c.})|{\rm i.c.})\times$$
$$[(B_\ell|(B_\ell|\exp\left(-\beta H_{\rm int}\right)|{\rm i.c.})|{\rm i.c.})(B_k|(B_k|\exp\left(-\beta H_{\rm int}\right)|{\rm i.c.})|{\rm i.c.})]^{-1/2}\Big] \tag{72}$$
$$=\frac{(B_k|(B_\ell|B)}{[(B_k|(B_k|B)(B_\ell|(B_\ell|B)]^{1/2}} \tag{73}$$
$$=\frac{\delta_{k,\ell}\lambda_{(B,k)}}{\left[\lambda_{(B,k)}\lambda_{(B,\ell)}\right]^{1/2}} \tag{74}$$
$$=\delta_{k,\ell}. \tag{75}$$

To recapitulate this sequence of inferences: an imaginary-time evolution operator $\exp(\ldots)$ appears on the right-hand-side of Eq. (72), and the action of this operator on the boundary state |i.c.)|i.c.) gives $|B)$ – up to a scalar factor – by definition. Hence, Eq. (73) follows from Eq. (72). Then Eq. (74) follows from the fact that $|B_k), |B_\ell)$ appear as orthonormal components in the expansion of $|B)$ in Eq. (70). Again, the definition of $|B)$ in terms of $H_{\rm int}$ provided by Eqs. (52) and (53) implies that,

$$\langle\Psi_{B_i}|\,\rho_{A\setminus B}\,|\Psi_{B_j}\rangle = \sum_{\alpha\beta\gamma}(B_\gamma|B_i)(B_\gamma|B_\beta)(B_\alpha|B_\beta)(B_\alpha|B_j)\frac{\lambda_\alpha\lambda_\beta\lambda_\gamma}{\sqrt{\lambda_i\lambda_j}} \tag{76}$$
$$= \delta_{ij}\lambda_i^2, \tag{77}$$

showing that $\rho_{A\setminus B}$ has the same spectrum as the operator B^2, defined in Eq. (68). An immediate implication is that the entanglement rank of the edge-picture ground state B is equal to the matrix rank of the bulk picture $\rho_{A\setminus B}$.

Equations (76) and (77) are shown in diagram form in Fig. 7. Performing the calculation to verify (76) in conventional notation, we construct a sequence of ever-finer lattice approximations of $\rho_{A\setminus B}$. Indexing the sequence by the integer m, we imagine that the lattice

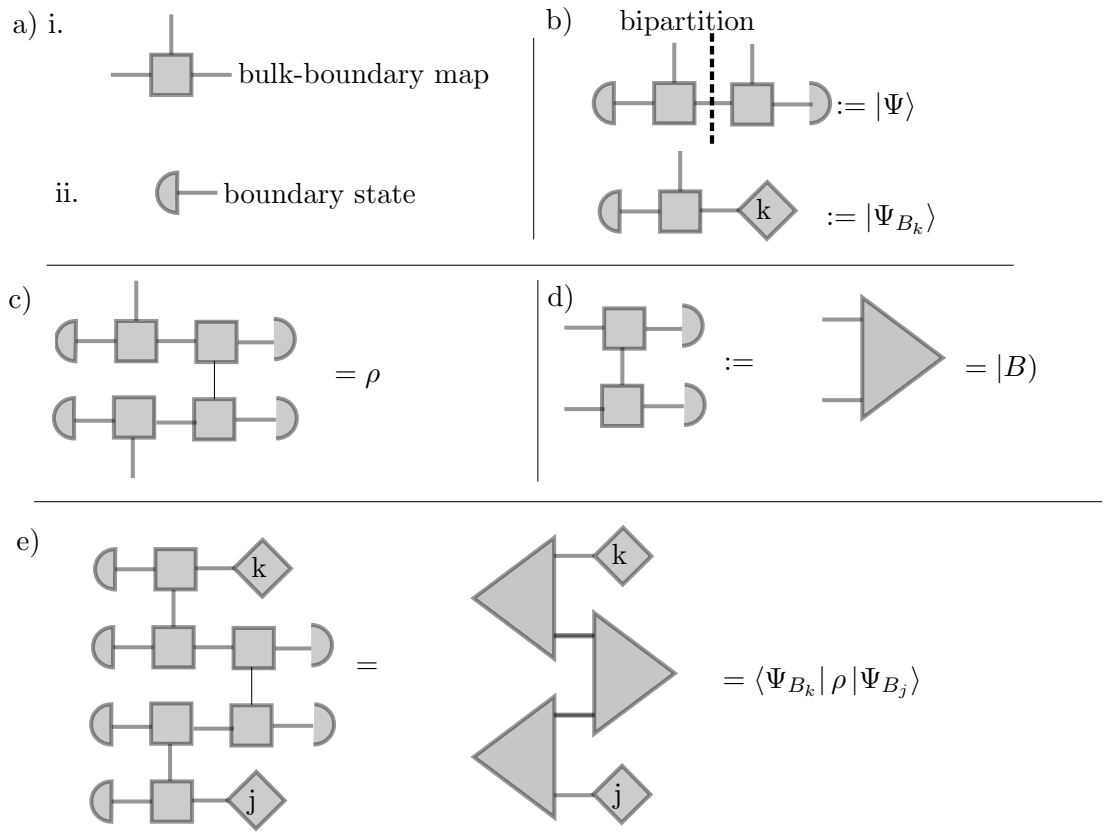

Figure 7: Equations (76), (77) in diagram from: (a) a simplified representation of the tensor expressions appearing in the definition of Spin-MR States, Eq. 1: i. the bulk boundary map, with vertical index corresponding to physical degrees of freedom and horizontal indices corresponding to auxillarly degrees of freedom; the two auxilary indices correspond to *in* states and *out* states of the imaginary time evolution operator; (b) the physical state $|\Psi\rangle$ formed by contracting the bulk-boundary map against auxillary *in* and *out* states; a bipartion of the physical degrees of freedom is formed by dividing imaginary time evolution into two equal intervals; the two uncontracted legs corresponds to the two parts of the bipartition; tensor network representation of the Schmidt basis on the left half of the bipartition, as defined in Eq. (71); (c) tensor network representation of the reduced density matrix on the left part; (d) the fixed point of the transfer matrix is the state $|B)$ in the auxiliary Hilbert space; (e) a matrix element in the $\{|\Psi_{B_k}\rangle\}$ basis expressed in terms of the components of $|B)$.

is divided into three parts: two sides of m rows of sites, each separated by the third part, which is the boundary itself. That is, there are m steps of discrete time evolution, then the boundary, then the remaining m steps of time evolution. To make this description precise, define the following functions:

$$Z^A(\beta, m, \ell, k) := (\text{i.c.}|(\text{i.c.}| \left(\exp\left(-\frac{\beta}{m} H_{\text{free}}\right) \bigotimes_{j=1}^{n} \left(\mathbb{I} + \frac{\beta}{m} \mu \rho_{(j)} \right) \right)^m |B_\ell^{(*)})|B_k), \tag{78}$$

$$Z^B(\beta, m, \ell, k) := (B_\ell^{(*)}|(B_k| \left(\bigotimes_{j=1}^{n} \left(\mathbb{I} + \frac{\beta}{m} \mu \rho_{(j)} \right) \exp\left(-\frac{\beta}{m} H_{\text{free}}\right) \right)^m |\text{i.c.})(\text{i.c.}). \tag{79}$$

Note that Z^A and Z^B each comprise m time steps, but that in Z^A the ordering of operators is such that the free Hamiltonian appears to the left of the interaction terms, whereas in Z^B the ordering is reversed. Between Z^A and Z^B there is therefore another free evolution operator, and this remaining operator represents the boundary.

Denote the sequence of lattice approximation, $\rho_{A\backslash B}(\epsilon, m, \beta)$, where $2\beta + \epsilon$ is the total imaginary time across the state. In the basis $\{|\Psi\rangle_{B_k}\}$, the components of each element of this sequence are:

$$\langle \Psi_{B_k} | \rho_{A\backslash B}(\epsilon, m, \beta) | \Psi_{B_\ell} \rangle = \tag{80}$$
$$\frac{\sum_{p,q,r,s} Z^A(\beta, m, \ell, p) Z^A(\beta, m, q, k) Z^B(\beta, m, r, s) (B_p^{(*)}|(B_q| \exp\left(-\epsilon H_{\text{free}}\right) |B_r^{(*)})|B_s)}{\sum_{k,\ell,p,q,r,s} Z^A(\beta, m, \ell, p) Z^A(\beta, m, q, k) Z^B(\beta, m, r, s) (B_p^{(*)}|(B_q| \exp\left(-\epsilon H_{\text{free}}\right) |B_r^{(*)})|B_s)}.$$

Commenting on the summand in the numerator: Z^B contains the dependencies of the traced out degrees of freedom (i.e., the unobserved part B of the system), the two Z^A contain the surviving degrees of freedom (the observable part A), and the remaining matrix element comes from a resolution of the identity that bridges the boundary between A and B. From the limits,

$$\lim_{m\to\infty} Z^A(\beta, m, \ell, k) = (\text{i.c.}|(\text{i.c.}| \exp(-\beta H_{\text{int}}|B_\ell^{(*)})|B_k), \tag{81}$$

$$\lim_{m\to\infty} Z^B(\beta, m, \ell, k) = (B_\ell|(B_k| \exp(-\beta H_{\text{int}}|\text{i.c.}^{(*)})(\text{i.c.}), \tag{82}$$

we then obtain Eq. (76).

4.4 Implications

The main technical result of this section is Eq. (77): what does this equation mean? Suppose that the ground state of the imaginary time evolution operator is maximally

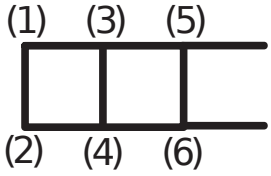

Figure 8: The state $|B)$ defined in Eq. (53) is the ground state of two coupled quantum spin chains; odd sites shown here belong to one chain, even the other; solid lines indicate nearest neighbour interactions.

entangled. Then Eq. (77) implies that the the bipartite entanglement entropy is maximal:

$$|B) = \frac{1}{\sqrt{N}} \sum_{i}^{N} |i)|i) \;\; \Rightarrow \;\; \rho_{A\setminus B} = \frac{1}{N} \sum_{i}^{N} |\Psi_{B_i}\rangle \langle \Psi_{B_i}| \,. \tag{83}$$

In this extreme case, all entanglement energies are degenerate. More generally, the introduction of the auxillarly state $|B)$ yields a *dynamical (re)description* — the H_{int} of equation Eq. (50) — of the entanglement in $|\Psi\rangle$. These dynamics are quasi-one-dimensional, describing two spin-chains coupled as shown in Fig. 8. The coupling across chains, sites (1)-(2), (2)-(3), and so on in the figure, is given by the local perturbation in Eq. (50). Approximate inferences about the entanglement entropy of the bipartite density matrix thus follow from the limiting behaviour of this perturbation. For example, in the case of the σ Ising Spin-MR state defined in Eq. (2), the introduction of a ferromagnetic coupling between two critical spin-chain should, heuristically, push $|B)$ off criticality and into a ferromagnetic phase. This heuristic reasoning then implies via Eq. (77) that the bipartite entanglement spectrum of the σ Spin-MR state should be two-fold degenerate. This argument is persued with greater rigor using the tools of Boundary CFT in the next chapter, tools which provide fixed-point approximations of $|B)$ in the IR limit.

5 Entanglement spectra: examples

This chapter applies the algorithm presented in Chapter 4 to two particular trial wavefunctions. First, the algorithm is tested by computing the entanglement spectrum of a known SPT ordered state, a special case discovered by Scaffidi and Ringle in [41]. The case is special because equivalent expressions for the wavefunction in both Spin-MR and group-cohomology formalisms are known, and in the latter form the state is provably SPT ordered. The algorithm yields the result that the entanglement spectrum of the test-state is indeed gapless, as the theory of SPT phases predicts. Second, the chapter calculates the entanglement-spectrum of the Ising Spin MR state introduced in Chapter 2, defined in Eq.(2). In that case, the reduced density matrix is a rank-two projector. Thus, the entanglement spectrum is degenerate, but the low-energy sector of the spectrum does not describe the critical Ising model, as might have been expected from the example of the Moore-Read ansatz. (The entanglement spectrum of the Moore-Read ansatz for the FQHE at five-halves filling does match the energy spectrum of the CFT out of which the ansatz is constructed [30].)

A technical tool used for the first time in this chapter is *Boundary CFT*. Boundary CFT enters to provide an IR fixed-point approximation to the ground-state $|B)$ of the transfer matrix of the boundary-picture theory, defined in Eq. (53) of Chapter 3. The state $|B)$ lives in the Hilbert-Space of a 1+1 D field theory and can be thought of as a boundary condition imposed on the (Heisenberg-picture) field operators of the theory. Boundary CFT describes all self-consistent boundary conditions on a CFT [9], and thus furnishes an expression for the fixed-point to which $|B)$ flows under renormalization. Only the fixed-point features of $|B)$ are needed in the limit that the system-size is large compared to the bulk correlation length. According to Boundary CFT, this fixed-point is a generalized coherent state and thus has nice properties, suited for analytic calculations. This use of Boundary CFT adapts to the bosonic case the treatment of fermionic MR states by Dubail, Read and Rezayi in [15].

5.1 Scaffidi-Ringel State and the free boson

Scaffidi and Ringel (*SR*) show that a set of SPT ordered trial wavefunctions are expressible as Spin-MR states. They give two descriptions of what, they argue, is the same state: one description in the language of symmetry group cohomology and the other in the Spin-MR language. They present numerical evidence that these descriptions are equivalent. Group cohomology is, like representation theory, a mathematical technique for studying symmetry groups via their group actions, specifically actions on abelian groups. And like representation theory, group cohomology provides a formalism for constructing symmetric wavefunctions, but one that naturally gives rise to exotic non-local properties [11].

To summarize SR's argument without rehearsing its details, their evidence is obtained by transforming a cohomology wavefunction into a statistical-mechanical partition function, then numerically computing the correlation length and central charge of this partition function. I take their Spin-MR description as given. Though Scaffidi and Ringle choose the details by trial-and-error, their trial-and-error search space is constrained by some general considerations that are needed for the calculations to follow. Their CFT is the free boson φ: the quantum theory of a scalar field φ that in the classical limit obeys the wave equation,

$$(\partial_t^2 - \partial_x^2)\varphi = 0. \tag{84}$$

The operator algebra of the free boson is rich, and in particular, other CFTs are identifiable as sub-algebras. There is a literature on classifying these sub-algebras that serves to frame the choices (on the right-hand-side of Eq. (1)) when constructing a Spin MR state. Among the free boson's operators, there is a special set of *scaling functions* ϕ that transform homogeneously under scale transformations $x \mapsto \lambda x$,

$$\phi(x) \mapsto \lambda^h \phi(\lambda x), \tag{85}$$

for constant h. The scaling functions are important in statistical mechanics because they can be measured macroscopically in the vicinity of a phase transition. A *primary field* is a scaling function that satisfies a generalization of Eq. (85) to all infinitesimal conformal transformations. The important point about primary fields for SR is the intuition that, to obtain Spin MR states in SPT phase, the CFT correlation functions on the right-hand-side of Eq. (1) ought to be expectations of products of primary fields, for reasons Moore and Read articulate in their seminal paper [33]. The primary fields in the free boson are remarkably easy to classify: they are $\partial\phi$ (think of the distribution of step-sizes in Brownian motion) and *vertex* operators of the form,

$$V_k(x) = e^{ik\varphi(x)}, \tag{86}$$

for real k. Thus, vertex operators of the free boson are a structured but also large set from which to construct a Spin MR state by numerical search, which is Scaffidi and Ringel's method.

Of the multiple examples SR consider in their paper, this chapter focuses on one example in detail, which SR construct as follows. The spins described by the SR state live on vertices of a hexagonal lattice. SR single out two sub-lattices B and C, as shown in Fig. 9(a). Occupation by a particle of a B site corresponds to the CFT operator $\cos(\varphi)$ and occupation of a C site to $\sin(\varphi)$. The fields $\cos(\varphi)$ and $\sin(\varphi)$ are linear combinations of vertex operators as defined in Eq. (86).

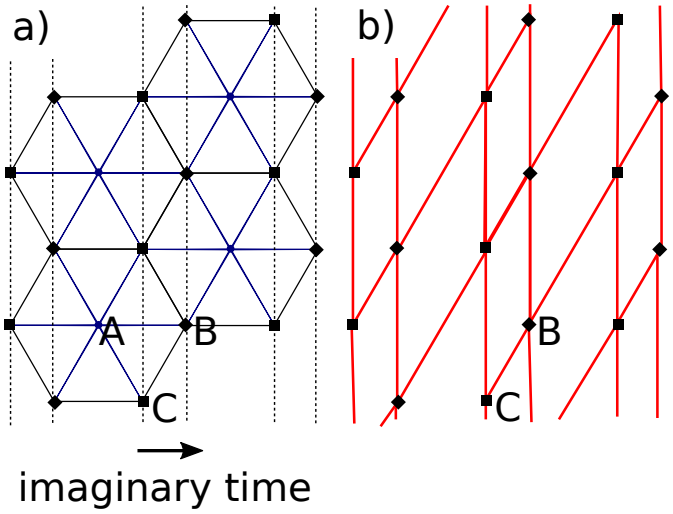

Figure 9: a) lattice geometry that Scaffidi and Ringel assume for their Spin MR state; the labels A, B, C mark three sub-lattices, the A sub-lattice is integrated out; imaginary time-slices indicated with dashed lines; b) an IR equivalent set of CFT correlators is obtained from a rectangular geometry as indicated by the red edges.

5.2 Scaffidi-Ringel State in the boundary-picture

To apply the algorithm of chapter 4, the SR state must be recast in the language of the boundary picture introduced in Chapters 1-3. Scaffidi and Ringel's hexagonal lattice structure is a relic of the cohomology formalism [11], and a square lattice (as shown in Fig. 9(b)) belongs to the same universality class in the continuum limit, when taking the limit such that the gas fugacity vanishes on the lattice scale.

Chapter 3 showed that, if the presence of a particle corresponds to the operator V, then the (boundary-picture) free field Hamiltonian that describes the (bulk-picture) square norm $\langle \Psi \mid \Psi \rangle$ is modified in the continuum limit by adding the term $-V^{(*)} \otimes V$. This same reasoning implies that if the operator corresponding to a particle alternates every time-step from V to Λ, then in the limit of vanishing time-step, the boundary picture Hamiltonian is modified by addition of the terms $-V^{(*)} \otimes V - \Lambda^{(*)} \otimes \Lambda$. In the continuum limit of the boundary picture, denote the degrees of freedom that correspond to $|\Psi\rangle$ by ϕ_A and likewise the degrees of freedom corresponding to $\langle \Psi|$ by ϕ_B. The continuum action S describing

the square norm of the SR state is therefore,

$$\begin{aligned} S &:= \int dxdt \ \ (\nabla\phi_A)^2 + (\nabla\phi_B)^2 - \mu^2\cos(\phi_A)\cos(\phi_B) - \mu^2\sin(\phi_A)\sin(\phi_B) \\ &= \int dxdt \left[\nabla\left(\frac{\phi_A - \phi_B}{\sqrt{2}}\right)\right]^2 + \left[\nabla\left(\frac{\phi_A + \phi_B}{\sqrt{2}}\right)\right]^2 - \mu^2\cos(\phi_A - \phi_B). \end{aligned} \tag{87}$$

with,

$$\langle\Psi \mid \Psi\rangle = \int \mathcal{D}[\phi_A]\mathcal{D}[\phi_B]e^{-S}. \tag{88}$$

The alternation between sine and cosine on the lattice has the consequence that a free sector decouples in the action. Label the decoupled variables,

$$\phi_{A'} = \frac{\phi_A - \phi_B}{\sqrt{2}}, \quad \phi_{B'} = \frac{\phi_A + \phi_B}{\sqrt{2}}. \tag{89}$$

Inspection of Eq. (87) shows that the field ϕ_A is in a massive Sine-Gordon phase whereas ϕ_B is in a Gaussian phase. Hence, the alternation of sine and cosine representations of particle insertion, though a lattice-scale detail, has an important effect on the continuum approximation. The free sector is (related to) the mechanism that creates long range entanglement. The free sector is also unobservable: there is no degree of freedom $\phi_{B'}$ in the physical Hilbert space. Instead, $\phi_{B'}$ has an interpretation in the tensor product of two copies of the physical Hilbert space, where it appears as the symmetric linear combination of particle creation operators, one in each space.

5.3 Infra-red fixed-point of the transfer matrix

This subsection finds an explicit expression for the IR fixed point of the ground state of the action in Eq. (87). The tool for making the fixed-point approximation is Boundary CFT. Boundary CFT is concerned with studying statistical mechanical systems at critical points that are subject to boundary conditions. In a Hilbert-space formulation of the statistical mechanical problem – in which an (arbitrary) axis of space is treated as imaginary time – the boundary condition is imposed by taking expectation values of operators with respect to a conformal boundary state. For example, Boundary CFT might study the critical Ising model on an infinite half-plane subject to the condition that all the spins at the boundary of the plane are parallel. A conformal boundary state $|X\rangle$ satisfies,

$$(L_n - \overline{L}_n)\,|X\rangle = 0, \tag{90}$$

for the Virasoro generators L_n of the CFT. This *Ishibashi condition* is a premise of the argument presented by Dubail, Read and Rezayi in [15]. These authors seek to show

that their fermionic MR-state has a gapless entanglement spectrum. In their case, the Aux Hilbert space is the space of holomorphic conformal blocks and $\text{Aux}^{(*)}$ the space of anti-holomorphic conformal blocks, so that the super-auxiliary $\text{Aux} \otimes \text{Aux}^{(*)}$ is the Hilbert space of the CFT. Therefore, under the mapping from states to operators, $|X\rangle \mapsto X$, (90) implies,

$$[L_n, X] = 0. \tag{91}$$

It follows from Shur's lemma that $X \propto \mathbb{I}$. By contrast, in the case of Spin-MR states, Aux is already the Hilbert space of a full CFT, and hence the Dubail, Read, Rezayi argument does not carry over to the bosonic case automatically: more work is needed to arrive at the analogous application of Shur's lemma, which this chapter now undertakes.

Returning to Eq. (87), Boundary CFT gives us an explicit formula for the fixed point state that pins $\phi_{A'}$ at a minima of the potential term in the action, namely, the Dirichlet boundary state $|D(\phi = 0))_A$. Hence, we take the fixed-point of the ground-state to be:

$$|B) := |D(\phi = 0))_{A'}|0)_{B'}, \tag{92}$$

where $|0)_{B'}$ is the Gaussian vacuum. I now offer a heuristic argument that the $|B)$ of Eq. (92) is the fixed-point to which the groundstate of the action in Eq. (87) flows (adapted from the argument in [15]). The state $|B)$ defined in Eq. (92) is invariant under scale transformations because its A' and B' factor states are so invariant, and the B' factor is the exact ground state of the B' terms in the boundary-picture action. Thus the true RG fixed point of the exact ground state must be a product state between A' and B' factor spaces and the B' factor must be the Gaussian vacuum. The authors of [15] guess that a Dirichlet boundary state is the fixed point of the exact wavefunction they investigate, and their reasoning is premised on the physically motivated guess that their exact wavefunction is in a charge-screening phase. In our case, charge screening is a demonstrable consequence of the definition of the action Eq. (87).

The language of "charge-screening" belongs to the Coulomb gas formalism of CFT and the observation that the N-point correlation function of vertex operators V in the free boson CFT are mathematically equivalent to the partition function of a canonical ensemble of N charged particles. The parameter k in Eq. (86) appears in the partition function formulation as the electric charge of V. A free boson correlator of vertex operators has the property that it vanishes unless the sum of all the k vanishes: the total charge of the gas is neutral.

5.4 Computing the leading eigenvalues of the reduced density matrix

This section infers the leading eigenvalues of the reduced density matrix on a bipartition. I show that the sufficient conditions for Schur's lemma are met, and it follows that the density matrix is proportional to the identity on the modules of the conformal algebra.

Recalling the recipe for computing entanglement spectra presented in the introduction to chapter 4, once an expression for the goundstate of the transfer matrix $|B)$ is obtained, the matrix elements of $\sqrt{\rho}$ (the square-root of the reduced density matrix) are given by the components of $|B)$ in the $\text{Aux} \otimes \text{Aux}^{(*)}$ product basis. This product basis factorizes the boundary-picture so that degrees of freedom associated with the physical bra and ket are explicitly distinct. With respect to the SR state, because the fixed-point Eq. (92) is a product of a Dirichlet state and the Gaussian vacuum, computing the transformation back to the $\text{Aux} \otimes \text{Aux}^{(*)}$ product basis is non-trivial. I need a name for the specific mapping from states to operators, so I denote it the *conjugating isomorphism* $\mathcal{I}_{\text{conj}}\big(|B)\big) := B$.

The result of this section is a density matrix $\mathcal{I}_{\text{conj}}\Big(|D(\phi=0)\rangle_{A'} |0\rangle_{B'} \Big)$ expressed as the limit of the action of a family of unitary operators $D^N(\xi)$ on the Gaussian vacuum $|0\rangle$:

$$\begin{aligned} &\mathcal{I}_{\text{conj}}\Big(|D(\phi=0)\rangle_{A'} |0\rangle_{B'} \Big) \\ = &\lim_{\substack{\epsilon \to 0 \\ N \to \infty}} \frac{1}{4^N} D_A^N\left(-\frac{1}{2\epsilon}\right) \mathcal{I}_{\text{conj}}\left(\exp\left\{ -\sum_{n=1}^{N} a_n^\dagger \tilde{b}_n^\dagger \right\} |0\rangle_{A_L} \langle 0|_{B_R} \right) D_A^N\left(\frac{1}{2\epsilon}\right). \end{aligned} \tag{93}$$

The subscripts L and R stand for left-moving and right-moving sectors, the notation for creation and annihilation operators is summarized in Table 1 and elaborated in detail below. The matrix $\mathcal{I}_{\text{conj}}\Big(|D(\phi=0)\rangle_{A'} |0\rangle_{B'} \Big)$ commutes with a representation of the Virasoro algebra and hence, by Shur's lemma, is proportional to the identity on each Verma module. The remainder of this section first derives Eq. (93) and then derives the commutation relations necessary to invoke Schur's lemma.

5.4.1 Changing to the bra-ket product basis

I change to the product basis by expressing the Dirichlet state in terms of creation and annihilation operators and then applying a Bogoliubov transformation. These wave-mode operators decompose the Aux and $\text{Aux}^{(*)}$ Hilbert spaces into the factor spaces of right-moving and left-moving free excitations. Write a_n for the right-moving annihilation operator of mode n on Aux and $\tilde{a}_n$ for the left-moving equivalent, likewise b_n and $\tilde{b}_n$ acting on $\text{Aux}^{(*)}$. Write a'_n for the right-moving annihilation operator of ϕ_A, likewise b'_n for the right-moving annihilation operator of ϕ_B, and let primes on the other operators carry the equivalent meaning. It is important to keep the meaning of these labels in mind and so Table 1 provides a summary. Denote the subspace of left-moving excitations X_L and of right-moving excitations X_R for $X \in \{A, B, A', B'\}$. Because the free boson has a zero-wave-number

	Annihilation operators			Annihilation operators	
D.O.F.	left-moving	right moving	D.O.F.	left-moving	right moving
A	a_n	$\tilde{a}_n$	A'	a'_n	$\tilde{a}'_n$
B	b_n	$\tilde{b}_n$	B'	b'_n	$\tilde{b}'_n$

Table 1: Annihilation operators on the Hilbert space $\mathrm{Aux} \otimes \mathrm{Aux}^{(*)}$. The pairs (A, B) and (A', B') are different tensor-product factorizations of the same Hilbert space, related by a $\pi/4$ rotation in Eq. (89). The preferred basis for extracting entanglement spectra from $|B)$ is (A, B); the expression for $|B)$ furnished by boundary CFT (Eq. (94)) is in the (A', B') basis.

mode, the full Hilbert space of the theory contains states that have an ambiguous propagation direction, but we can simply resolve the ambiguity by defining a right-mover as any mode with $k > 0$ and a left-mover as any mode with $k \leq 0$.

The expression for the Dirichlet boundary state is then,

$$|D(\phi = 0))_{A'} = \exp\left\{ -\sum_n {a'_n}^\dagger \tilde{a}'^\dagger_n \right\} |0)_{A'_L} |0)_{A'_R}. \tag{94}$$

The route to Shur's lemma from Eq. (94) is to expand the primed operators in terms of unprimed and to compute the action of the operator on the right-hand-side of Eq. (94) in the $\mathrm{Aux} \otimes \mathrm{Aux}^{(*)}$ basis. The calculation is simplified by finding a unitary operator whose action on the A' vacuum gives $|D(\phi = 0))_{A'}$, much like a quantum-optics displacement operator would act on a single mode. The result is then an expression in terms of the action of fully factorized unitary operators on a product of Ishibashi state in the $\mathrm{Aux} \otimes \mathrm{Aux}$ product-basis.

A unitary operator with equivalent vacuum action to the exponential appearing in Eq. (94) is found by identifying a representation of the algebra $\mathfrak{su}(1,1)$ in the product of right and left-moving operators. This algebra generates symmetries of the harmonic oscillator and thus is closely related to quantum coherent states. Let,

$$K_{-,n} := a_n \tilde{a}_n, \quad K_{+,n} := a_n^\dagger \tilde{a}_n^\dagger, \quad K_{0,n} := \frac{1}{2}(a_n a_n^\dagger \tilde{a}_n \tilde{a}_n^\dagger + 1), \tag{95}$$

then these operators satisfy the $\mathfrak{su}(1,1)$ commutation relations,

$$[K_{0,n}, K_{\pm,n}] = \pm K_{\pm,n}, \quad [K_{-,n}, K_{+,n}] = 2K_{0,n}. \tag{96}$$

These commutation relations can be shown to imply the existence of a one complex parameter family of unitary operators [39],

$$D_n(\xi) := \exp\left\{ \xi K_{+,n} - \xi^* K_{-,n} \right\}, \tag{97}$$

that decompose as,

$$D_n(\xi) = \exp\left\{\zeta K_{+,n}\right\} \exp\left\{\eta K_{0,n}\right\} \exp\left\{\zeta' K_{-,n}\right\}, \tag{98}$$

with

$$\zeta = \tanh|\xi| e^{i\varphi}, \quad \eta = -\ln(1-|\zeta|^2), \quad \zeta' = -\zeta^*. \tag{99}$$

It is this disentangling relationship, Eqs. (97) and (98), that makes the computation of $|B)$ in the A, B basis possible. I seek to show that,

$$\exp\left\{-\sum_n {a'_n}^\dagger \tilde{a}'^\dagger_n\right\} |0)_{A'_L} |0)_{A'_R} = \lim_{\xi\to-\infty} \prod_{n=1}^{\infty} D_n(\xi) |0)_{A'_L} |0)_{A'_R}. \tag{100}$$

Substituting the expression on the right-hand-side of Eq. (100) for the left-hand-side is useful because the Gaussian vacuum is an eigenstate of $K_{0,n}$ and $K_{-,n}$ for all n:

$$K_{-,n} |0\rangle = 0, \tag{101}$$

$$K_{0,n} |0\rangle = |0\rangle. \tag{102}$$

Referring back to the parameters appearing in Eq (98), let us suppose finite $\xi = -1/\epsilon$ and then take the limit $\epsilon \to 0,\ \zeta \to -1$. Then,

$$|D(\varphi=0)\rangle_{A'} |0\rangle_{B'} = \lim_{\substack{\epsilon\to 0 \\ N\to\infty}} \exp\left\{-\tanh(1/\epsilon) \sum_{n=1}^{N} a_n^{\dagger\prime} \tilde{a}_n^{\dagger\prime}\right\} |0\rangle_{A_L} |0\rangle_{A_R} |0\rangle_{B_L} |0\rangle_{B_R}. \tag{103}$$

Now we can substitute for the exponential occurring on the right hand side of Eq. (103) the product $\prod_n D_n(1/\epsilon)$,

$$\begin{aligned}
&\exp\left\{-\tanh(1/\epsilon) \sum_{n=1}^{N} a_n^{\dagger\prime} \tilde{a}_n^{\dagger\prime}\right\} |0\rangle_{A_L} |0\rangle_{A_R} |0\rangle_{B_L} |0\rangle_{B_R} \\
&= \left(1-\tanh^2[1/\epsilon]\right)^N \exp\left\{-\tanh(1/\epsilon) \sum_{n=1}^{N} a_n^{\dagger\prime} \tilde{a}_n^{\dagger\prime}\right\} \\
&\quad \times \exp\left\{-\ln\left[1-\tanh^2(1/\epsilon)\right] \sum_{n=1}^{N} \frac{1}{2}(a'_n a'^\dagger_n \tilde{a}'_n \tilde{a}'^\dagger_n + 1)\right\} \\
&\quad \times \exp\left\{\tanh(1/\epsilon) \sum_{n=1}^{N} a'_n \tilde{a}'_n\right\} |0\rangle_{A_L} |0\rangle_{A_R} |0\rangle_{B_L} |0\rangle_{B_R} \qquad (104) \\
&= \left(1-\tanh^2[1/\epsilon]\right)^N \exp\left\{-\frac{1}{\epsilon} \sum_{n=1}^{N} \left(a_n^{\dagger\prime} \tilde{a}_n^{\dagger\prime} - a'_n \tilde{a}'_n\right)\right\} |0\rangle_{A_L} |0\rangle_{A_R} |0\rangle_{B_L} |0\rangle_{B_R}. \qquad (105)
\end{aligned}$$

Above, Eq. (104) inserts an exponential in $K_{-,n}$ that acts as the identity on the vacuum, per the eigenvalue relation Eq. (101), and an exponential in $K_{0,n}$, of which the vacuum is an eigenvector. The prefactor appearing on the right-hand side of Eq. (104) is the inverse of the vacuum eigenvalue of the exponentiated $K_{0,n}$ and thus the prefactor cancels what would otherwise be the effect of inserting that operator. Collecting the three exponentials appearing on the right-hand-side of Eq. (104) according to Eqs. (97) and (98) results in Eq. (105). We now rewrite the right-hand-side of Eq. (105) in terms of mode operators in the A, B basis. After the change of basis, we again use the eigenvalue relation Eq. (102) to reabsorb the prefactor $\left(1-\tanh^2[1/\epsilon]\right)^N$; the asymptotic form this prefactor is $\exp[N/\epsilon]$ and hence rapidly vanishes in the limit we are taking. To make the change of basis, recall the definition of primed operators:

$$a'_n = \frac{1}{\sqrt{2}}(a_n + b_n), \quad b'_n = \frac{1}{\sqrt{2}}(a_n - b_n), \tag{106}$$

where a is an A_L boson annihilation operator and b is a B_L boson annihilation operator: likewise is a' to A'_L and b' to B'_L, and so too operators dressed with tildes to the right moving Hilbert spaces. Expanding the exponent appearing on the right-hand-side of Eq. (105),

$$\begin{aligned}
&\exp\left\{-\frac{1}{\epsilon}\sum_{n=1}^{\infty}\left(a_n^{\dagger\prime}\tilde{a}_n^{\dagger\prime} - a'_n\tilde{a}'_n\right)\right\}|0\rangle_{A_L}|0\rangle_{A_R}|0\rangle_{B_L}|0\rangle_{B_R} \\
=&\exp\left\{-\frac{1}{2\epsilon}\sum_{n=1}^{\infty}\Big([a_n^\dagger\tilde{a}_n^\dagger - a_n\tilde{a}_n] + [b_n^\dagger\tilde{b}_n^\dagger - b_n\tilde{b}_n]\right. \\
&\qquad\left.+ [a_n^\dagger\tilde{b}_n^\dagger - a_n\tilde{b}_n] + [b_n^\dagger\tilde{a}_n^\dagger - b_n\tilde{a}_n]\Big)\right\}|0\rangle_{A_L}|0\rangle_{A_R}|0\rangle_{B_L}|0\rangle_{B_R}\,.
\end{aligned} \tag{107}$$

On the right-hand-side of Eq. (107), square brackets are used to group terms that are patterned after the definition of the displacement operator in Eq. (97). The notable difference in Eq. (107) as compared with Eq. (97) is the presence of terms that mix A and B operators. These mixing terms build the entanglement between the A and B degrees of freedom (in the boundary picture) that entail a gapless entanglement spectrum (in the bulk picture). From here, we look to factorize the exponential appearing on the right-hand-side of Eq. (107) as a product of displacement operators. To apply the Baker-Campbell-Hausdorff formula to achieve this factorization, we must verify that the first four terms in the exponent commute with the last four, taking the verifying computation in stages. First, compute the following commutator of pure A terms with cross terms that mix A and B,

$$[a_n^\dagger\tilde{a}_n^\dagger - a_n\tilde{a}_n, a_n^\dagger\tilde{b}_n^\dagger - a_n\tilde{b}_n] = -[a_n^\dagger, a_n]\tilde{a}_n^\dagger\tilde{b}_n - [a_n, a_n^\dagger]\tilde{a}_n\tilde{b}_n^\dagger = \tilde{a}_n^\dagger\tilde{b}_n - \tilde{a}_n\tilde{b}_n^\dagger. \tag{108}$$

Computing the same with the other pair of cross terms,

$$[a_n^\dagger\tilde{a}_n^\dagger - a_n\tilde{a}_n, b_n^\dagger\tilde{a}_n^\dagger - b_n\tilde{a}_n] = -[\tilde{a}_n^\dagger, \tilde{a}_n]a_n^\dagger b_n - [\tilde{a}_n, \tilde{a}_n^\dagger]a_n b_n^\dagger = a_n^\dagger b_n - a_n b_n^\dagger, \tag{109}$$

And now consider commutators with pure B terms,

$$[b_n^\dagger \tilde{b}_n^\dagger - b_n \tilde{b}_n, a_n^\dagger \tilde{b}_n^\dagger - a_n \tilde{b}_n] = -[\tilde{b}_n^\dagger, \tilde{b}_n] b_n^\dagger a_n - [\tilde{b}_n, \tilde{b}_n^\dagger] a_n^\dagger b_n = -(a_n^\dagger b_n - a_n b_n^\dagger), \tag{110}$$

and,

$$[b_n^\dagger \tilde{b}_n^\dagger - b_n \tilde{b}_n, b_n^\dagger \tilde{a}_n^\dagger - b_n \tilde{a}_n] = -[b_n^\dagger, b_n] \tilde{b}_n^\dagger \tilde{a}_n - [b_n, b_n^\dagger] \tilde{b}_n \tilde{a}_n^\dagger = -(\tilde{a}_n^\dagger \tilde{b}_n - \tilde{a}_n \tilde{b}_n^\dagger). \tag{111}$$

Comparing the right-hand-side of Eq. (108) with Eq. (110), and of Eq. (109) with Eq. (111), the commutators of pure A terms cancel the commutators of pure B terms. From this cancellation, it follows that,

$$[a_n^\dagger \tilde{a}_n^\dagger - a_n \tilde{a}_n + b_n^\dagger \tilde{b}_n^\dagger - b_n \tilde{b}_n,\ a_n^\dagger \tilde{b}_n^\dagger - a_n \tilde{b}_n + b_n^\dagger \tilde{a}_n^\dagger - b_n \tilde{a}_n] = 0. \tag{112}$$

From Eq. (112) and the Campbell-Baker-Hausdorff formula, we obtain,

$$\begin{aligned}
&\exp\left\{-\frac{1}{2\epsilon}\sum_{n=1}^{N}\left(a_n^\dagger \tilde{a}_n^\dagger - a_n \tilde{a}_n + b_n^\dagger \tilde{b}_n^\dagger - b_n \tilde{b}_n + a_n^\dagger \tilde{b}_n^\dagger - a_n \tilde{b}_n + b_n^\dagger \tilde{a}_n^\dagger - b_n \tilde{a}_n\right)\right\} \\
&= \exp\left\{-\frac{1}{2\epsilon}\sum_{n=1}^{N} a_n^\dagger \tilde{a}_n^\dagger - a_n \tilde{a}_n\right\} \exp\left\{-\frac{1}{2\epsilon}\sum_{n=1}^{N} b_n^\dagger \tilde{b}_n^\dagger - b_n \tilde{b}_n\right\} \\
&\quad \times \exp\left\{-\frac{1}{2\epsilon}\sum_{n=1}^{N} a_n^\dagger \tilde{b}_n^\dagger - a_n \tilde{b}_n\right\} \exp\left\{-\frac{1}{2\epsilon}\sum_{n=1}^{\infty} b_n^\dagger \tilde{a}_n^\dagger - b_n \tilde{a}_n\right\}.
\end{aligned} \tag{113}$$

The next move is to recast the exponentials on the right-hand-side of Eq. (113) in the form of the expression for Dirichlet boundary states, Eq. (92),

$$\begin{aligned}
&\exp\left\{-\frac{1}{2\epsilon}\sum_{n=1}^{N} a_n^\dagger \tilde{b}_n^\dagger - a_n \tilde{b}_n\right\} |0\rangle_{A_L} |0\rangle_{B_R} \\
&= \exp\left\{-\tanh(1/2\epsilon)\sum_{n=1}^{N} a_n^\dagger \tilde{b}_n^\dagger\right\} \exp\left\{-\ln\left[1-\tanh^2(1/2\epsilon)\right]\sum_{n=1}^{N}\frac{1}{2}(a_n a_n^\dagger \tilde{b}_n \tilde{b}_n^{\dagger\prime} + 1)\right\} \\
&\quad \times \exp\left\{\tanh(1/2\epsilon)\sum_{n=1}^{N} a_n \tilde{b}_n\right\} |0\rangle_{A_L} |0\rangle_{B_R}
\end{aligned} \tag{114}$$

$$= \left(1-\tanh^2[1/2\epsilon]\right)^{-N} \exp\left\{-\tanh(1/2\epsilon)\sum_{n=1}^{N} a_n^\dagger \tilde{b}_n^\dagger\right\} |0\rangle_{A_L} |0\rangle_{B_R}. \tag{115}$$

Pausing to consolidate these intermediate results: together, Eqs. (103), (105), (113) and (115) imply the expression,

$$\begin{aligned}|D(\varphi=0)\rangle_{A'}\,|0\rangle_{B'} = \lim_{\substack{\epsilon\to 0\\ N\to\infty}} & \left(\frac{1-\tanh^2[1/\epsilon]}{\left(1-\tanh^2[1/\epsilon]\right)^2}\right)^N \exp\left\{-\frac{1}{2\epsilon}\sum_{n=1}^{N} a_n^\dagger \tilde{a}_n^\dagger - a_n\tilde{a}_n\right\} \\ & \times \exp\left\{-\frac{1}{2\epsilon}\sum_{n=1}^{N} b_n^\dagger \tilde{b}_n^\dagger - b_n\tilde{b}_n\right\} \exp\left\{-\tanh(1/2\epsilon)\sum_{n=1}^{N} a_n^\dagger \tilde{b}_n^\dagger\right\} \\ & \times \exp\left\{-\tanh(1/2\epsilon)\sum_{n=1}^{N} \tilde{a}_n^\dagger b_n^\dagger\right\} |0\rangle_{A_L}\,|0\rangle_{A_R}\,|0\rangle_{B_L}\,|0\rangle_{B_R}\,. \end{aligned} \tag{116}$$

The $\epsilon \to 0$ limiting value of the overall prefactor appearing on the right-hand-side of Eq. (116) is,

$$\lim_{\epsilon\to 0} \frac{1-\tanh^2(1/\epsilon)}{\left[1-\tanh^2(1/2\epsilon)\right]^2} = \frac{1}{4}. \tag{117}$$

Thus, we have found, starting from Eq. (92), a simplified expression for the fixed-point of the boundary picture ground-state in the $\mathrm{Aux}\otimes\mathrm{Aux}^*$ product basis (the un-primed basis):

$$\begin{aligned}|D(\phi=0)\rangle_{A'}\,|0\rangle_{B'} = \lim_{\substack{\epsilon\to 0\\ N\to\infty}} & \frac{1}{4^N}\prod_{n=1}^{N} D_{n,A}\left(-\frac{1}{2\epsilon}\right) D_{n,B}\left(-\frac{1}{2\epsilon}\right) \\ & \times \exp\left\{-\sum_{n=1}^{N} a_n^\dagger \tilde{b}_n^\dagger\right\} \exp\left\{-\sum_{n=1}^{N} b_n^\dagger \tilde{a}_n^\dagger\right\} |0\rangle_{A_L}\,|0\rangle_{A_R}\,|0\rangle_{B_L}\,|0\rangle_{B_R}\,. \end{aligned} \tag{118}$$

The final result of the calculation in this section is approaching, and the remaining step is to prove a property of the states created by the action of the mixed exponentials in Eq. (118) on vacua, namely,

$$\left(a_k - \tilde{b}_k\right) \exp\left\{-\sum_{n=1}^{N} a_n^\dagger \tilde{b}_n^\dagger\right\} |0\rangle_{A_L}\,|0\rangle_{B_R} = 0, \tag{119}$$

$$(\tilde{a}_k - b_k) \exp\left\{-\sum_{n=1}^{N} \tilde{a}_n^\dagger b_n^\dagger\right\} |0\rangle_{A_R}\,|0\rangle_{B_L} = 0. \tag{120}$$

Let us verify Eq. (119) explicitly; Eq. (120) follows from nearly identical reasoning.

$$
\begin{aligned}
&\left(a_k - \tilde{b}_k\right) \exp\left\{-\sum_{n=1}^{N} a_n^\dagger \tilde{b}_n^\dagger\right\} |0\rangle_{A_L} |0\rangle_{B_R} \\
&= \left(a_k - \tilde{b}_k\right) \exp\left\{-a_k^\dagger \tilde{b}_k^\dagger\right\} |0\rangle_{A_L} |0\rangle_{B_R} && (121)\\
&= \left(a_k - \tilde{b}_k\right) \sum_{n=0}^{N} (-1)^n |n_k\rangle_A |n_k\rangle_{\tilde{B}} && (122)\\
&= \sum_{n=1}^{N} (-1)^n (n-n)\, n\, |(n-1)_k\rangle_{A_L} |(n-1)_k\rangle_{B_R} && (123)\\
&= 0, && (124)
\end{aligned}
$$

where Eq. (121) follows from the fact that $(a_k - \tilde{b}_k)$ commute past $a_n^\dagger \tilde{b}_n^\dagger$ for all $n \neq k$, and Eq. (122) follows by expanding the exponential. The notation $|n_k\rangle$ means that mode k has occupation number n.

5.4.2 Transforming the boundary state into the density matrix

The implication of Eqs. (119) and (120) on the entanglement spectrum of the SR state is to be found by comparing the form of Eqs. (119) and Eqs. (120) with the Ishibashi condition, Eq. (90). Let us restate the canonical isomorphism $\mathcal{I}_{canon}$ between states in $\mathrm{Aux} \otimes \mathrm{Aux}^{(*)}$ and operators on Aux. Let $\Psi_{ijk\ell}$ be any complex valued four-indexed tensor. Then define,

$$
\begin{aligned}
&\mathcal{I}_{\mathrm{canon}} : \mathrm{Aux} \otimes \mathrm{Aux}^{(*)} \to \mathrm{End}(\mathrm{Aux}); \\
&\mathcal{I}_{\mathrm{canon}} \left(\sum_{ijk\ell} \Psi_{ijk\ell} a_i^\dagger \tilde{a}_j^\dagger b_k \tilde{b}_\ell^\dagger |0\rangle_{A_L} |0\rangle_{A_R} |0\rangle_{B_L} |0\rangle_{B_R} \right) = \sum_{ijk\ell} \Psi_{ijk\ell} a_i^\dagger \tilde{a}_j^\dagger |0\rangle_{A_L} |0\rangle_{A_R} \langle 0|_{A_L} \langle 0|_{A_R} a_k \tilde{a}_\ell .
\end{aligned} \tag{125}
$$

Now, Eqs. (119) and (120) imply that, for all k,

$$
a_k \mathcal{I}_{\mathrm{canon}} \left(\exp\left\{-\sum_{n=1}^{N} a_n^\dagger \tilde{b}_n^\dagger\right\} |0\rangle_{A_L} |0\rangle_{B_R} \right) - \mathcal{I}_{\mathrm{canon}} \left(\exp\left\{-\sum_{n=1}^{N} a_n^\dagger \tilde{b}_n^\dagger\right\} |0\rangle_{A_L} |0\rangle_{B_R} \right) \tilde{a}_k = 0, \tag{126}
$$

$$
\tilde{a}_k \mathcal{I}_{\mathrm{canon}} \left(\exp\left\{-\sum_{n=1}^{N} b_n^\dagger \tilde{a}_n^\dagger\right\} |0\rangle_{A_L} |0\rangle_{B_R} \right) - \mathcal{I}_{\mathrm{canon}} \left(\exp\left\{-\sum_{n=1}^{N} b_n^\dagger \tilde{a}_n^\dagger\right\} |0\rangle_{A_L} |0\rangle_{B_R} \right) \tilde{a}_k = 0. \tag{127}
$$

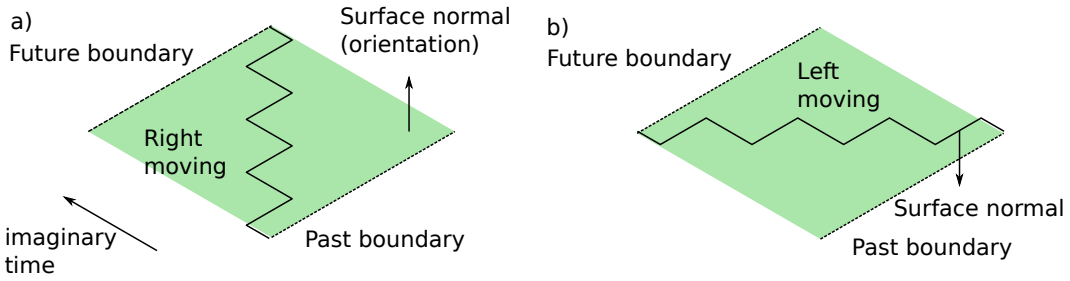

Figure 10: Geometric interpretation of the conjugating isomorphism defined by Eq. (128).

These Eqs. (126) and (127) are examples of the commutation relation Eq. (91), except that the operators acting on $\mathcal{I}(\cdot)$ from the left are in a left-moving representation and the operators acting from the right are in a right-moving representation. We can thus define an isomorphism that interchanges the left and right sub-spaces:

$$\mathcal{I}_{\text{conj}} : \text{Aux} \otimes \text{Aux}^{(*)} \to \text{End}(\text{Aux});$$

$$\mathcal{I}_{\text{conj}}\left(\sum_{ijk\ell} \Psi_{ijk\ell} a_i^\dagger \tilde{a}_j^\dagger b_k \tilde{b}_\ell^\dagger \left|0\right\rangle_{A_L} \left|0\right\rangle_{A_R} \left|0\right\rangle_{B_L} \left|0\right\rangle_{B_R}\right) = \sum_{ijk\ell} \Psi_{ijk\ell} a_i^\dagger \tilde{a}_j^\dagger \left|0\right\rangle_{A_L} \left|0\right\rangle_{A_R} \left\langle 0\right|_{A_L} \left\langle 0\right|_{A_R} \tilde{a}_k a_\ell. \tag{128}$$

Under this *conjugating* isomorphism, the equivalents of Eqs.(126) and (127) are:

$$\left[a_k, \mathcal{I}_{\text{conj}}\left(\exp\left\{-\sum_{n=1}^{N} a_n^\dagger \tilde{b}_n^\dagger\right\} \left|0\right\rangle_{A_L} \left|0\right\rangle_{B_R}\right)\right] = 0, \tag{129}$$

$$\left[\tilde{a}_k, \mathcal{I}_{\text{conj}}\left(\exp\left\{-\sum_{n=1}^{N} b_n^\dagger \tilde{a}_n^\dagger\right\} \left|0\right\rangle_{A_L} \left|0\right\rangle_{B_R}\right)\right] = 0. \tag{130}$$

The conjugating isomorphism interpreted as an automorphism on the Hilbert space of the CFT has the geometric interpretation of a mirror reflection about the complex plane in which the CFT of the boundary picture is defined, i.e., imagining a normal vector out of the plane, the reflection that reverses the direction of the normal vector, as shown in Fig. 10.

I have defined the action of $\mathcal{I}_{\text{conj}}$ on states, but to get to Schur's lemma, I also need a definition of its action on operators. That definition can be given implicitly as the completion of the commutative diagram shown in Table 2. Suppose any operator $\phi \in \text{End}(\text{Aux}^{(*)})$: there exists a mapping $\mathcal{I}_{\text{conj}} : \text{End}\big(\text{Aux}^{(*)}\big) \to \text{End}(\text{Aux})$ so that the diagram shown in Table 2 commutes. As an operator on End(Aux), $\mathcal{I}_{\text{conj}}(\phi)$ acts by multiplication

$$\begin{array}{ccc} \mathrm{End}(\mathrm{Aux}) & \underset{\mathcal{I}_{\mathrm{conj}}(\phi)}{\longrightarrow} & \mathrm{End}(\mathrm{Aux}) \\ \mathcal{I}_{\mathrm{conj}}\uparrow & & \mathcal{I}_{\mathrm{conj}}\uparrow \\ \mathrm{Aux}\otimes\mathrm{Aux}^{(*)} & \underset{\mathrm{id.}\otimes\phi}{\longrightarrow} & \mathrm{Aux}\otimes\mathrm{Aux}^{(*)} \end{array}$$

Table 2: Commuting diagram that defines the mapping $\mathcal{I}_{\mathrm{conj}}(\phi)$ as it appears in Eq. (133). The action of $\mathcal{I}_{\mathrm{conj}}(\phi)$ on elements of End(Aux) is defined by Eq. (131).

from the right:

$$\mathcal{I}(\phi)\,[X] := X\cdot\mathcal{I}(\phi), \quad \forall\ \phi, X\in \mathrm{End}(\mathrm{Aux}). \tag{131}$$

Let us adopt the abbreviation,

$$D^N_{X,n} := \prod_{n=1}^{N} D_{X,n}(\xi), \quad X\in\{A,B\}. \tag{132}$$

It then follows from the implicit definition of $\mathcal{I}$ in Table. 2 that,

$$\mathcal{I}_{\mathrm{conj}}\left(D^N_B\left(-\frac{1}{2\epsilon}\right)\right) = D^N_A\left(\frac{1}{2\epsilon}\right). \tag{133}$$

The commutation relations below then follow from Eqs. (129) and (130), for all $k\leq N$:

$$\left[D^N_A\left(-\frac{1}{2\epsilon}\right)a_k D^N_A\left(\frac{1}{2\epsilon}\right), \mathcal{I}_{\mathrm{conj}}\Big(\left|D(\phi=0)\right\rangle_{A'}\left|0\right\rangle_{B'}\Big)\right] = 0, \tag{134}$$

$$\left[D^N_A\left(-\frac{1}{2\epsilon}\right)\tilde{a}_k D^N_A\left(\frac{1}{2\epsilon}\right), \mathcal{I}_{\mathrm{conj}}\Big(\left|D(\phi=0)\right\rangle_{A'}\left|0\right\rangle_{B'}\Big)\right] = 0. \tag{135}$$

That Eqs. (129) and (130) imply Eqs. (134) and (135) follows from the elementary operator identity:

$$[U^\dagger X U, U^\dagger Y U] = U^\dagger [X,Y] U, \tag{136}$$

letting X, Y be any matrices of the same dimension and U be any unitary matrix of the same dimension again. The relevant unitary operator is D^N_A and, The commutative diagram Table 2 ensures that Eq. (93) is equivalent to Eq. (118).

Having reached Eqs. (134) and (135) we are at the threshold of applying Shur's lemma. The representation theory of the set of operators $\{a_k, \tilde{a}_k\}$ generalizes the raising and lowering

operators of the quantum harmonic oscillator. An important respect in which the former theory is more general is that its Hilbert space contains infinitely many vacuum states. These vacuum states correspond, in the language of electric circuits, to the infinitely many possible DC offsets and drifts, atop of which ride AC the excitations that the $\{a_k^\dagger, \tilde{a}_k^\dagger\}$ create. The Hilbert space of the theory therefore breaks up into towers of states, *Verma modules*, each generated from a different vacuum state. The operators $\{D_A^N a_k D_A^{N-1}, D_A^N \tilde{a}_k D_A^{N-1}\}$ appearing in Eqs.(134), (135), obey the same algebra as the $\{a_k, \tilde{a}_k\}$ and hence structure the Hilbert space into Verma modules, let them be called *squeezed* modules to contrast with *un-squeezed*. The relation between squeezed and un-squeezed modules is not important for our purpose; rather, our concern is the spectrum of $\mathcal{I}_{\text{conj}}\left(|D(\phi=0)\rangle_{A'} |0\rangle_{B'} \right)$. From Schur's lemma and Eqs. (134),(135) it follows that $\mathcal{I}_{\text{conj}}\left(|D(\phi=0)\rangle_{A'} |0\rangle_{B'} \right)$ is proportional to the identity on each of the squeezed modules, and in particular that there exists one squeezed module corresponding to the largest magnitude eigenvalue, and that this eigenvalue is degenerate on that module. Hence, the spectrum of $\mathcal{I}_{\text{conj}}\left(|D(\phi=0)\rangle_{A'} |0\rangle_{B'} \right)$ is gapless and the entanglement spectrum of the reduced density matrix of $|\Psi\rangle$ on a bipartition is gapless.

In summary, the SR state is SPT ordered by construction [41] , and the method for calculating entanglement spectra developed in Chapter 4, which here has been applied to the SR stater, gives results consistent with non-trivial SPT order.

5.5 The Ising model spin-operator state

Chapter 2 introduced a Spin MR state $|\Psi\rangle$ that took the critical Ising model as its CFT and the spin operator σ as the field corresponding to particle insertion. The definition of $|\Psi\rangle$ is given in Eq. (2). Chapter 2 mounted an argument to show that this Ising Spin MR state might plausibly exhibit SPT order. Here, the algorithm of chapter 4 is applied to show that the entanglement spectrum of this state is degenerate: the reduced density matrix is a projector onto a two-dimensional subspace of the physical Hilbert space.

By way of prefacing the technical detail, consider the following heuristic argument that the entanglement spectrum of $|\Psi\rangle$ defined in Eq. (2) is degenerate. We seek the IR fixed point of the ground state of a Hamiltonian that describes the dynamics of two copies of the 1+1D critical transverse field Ising model interacting with each other via a local perturbation. The tensor network picture allows us to imagine two spin-chains that resemble the two legs of a ladder, with the rungs of the ladder the perturbing interaction. The perturbing interaction is ferromagnetic. The ferromagnetic interaction tips the two critical Ising models over into a ferromagnetic phase and the hence the IR fixed point is the superposition of two states,

one all-spins-up, the other all spins down. This ground state in hand, we need to map it via the canonical isomorphism to an operator on the Ising model Hilbert space. This operator is a projector onto the all-spins-up and all-spins-down subspace.

We again approximate the ground-state of the boundary-picture Hamiltonian using Boundary CFT. The boundary-picture Hilbert space is the tensor product of two critical Ising models. In the continuum limit, this doubled Ising-model is equivalent to the the orbifold boson, following the strategy for Ising model calculations presented in [37] and [38] (for a derivation of the "bosonized" description from the discrete lattice model, see [4]). The orbifold is obtained from the free boson by first identifying $\varphi \equiv \varphi + 2\pi r$, which is the compact boson of radius r, and then identifying $\varphi \equiv -\varphi$ on the fundamental domain $[-\pi r, \pi r]$. The field content of the orbifold is studied in [14]. There is a family of primary fields in the orbifold theory indexed by the integer k that are each a superposition of compact boson vertex operators,

$$\phi_k = \frac{1}{2}\left(e^{ik\varphi/2} - e^{-ik\varphi/2}\right). \tag{137}$$

The field $\phi_1 = \cos(\varphi/2)$ is the most singular term in the OPE of the spin operators σ_1, σ_2 from the two Ising models and has conformal dimensions $\left(\frac{1}{8}, \frac{1}{8}\right)$. The partition function of the perturbed theory is thus formally the series in μ,

$$Z_{\text{int}} \equiv \left\langle \exp\left(-\mu \int d^2x \ \cos(\varphi(x)/2)\right)\right\rangle_{\text{orb}}. \tag{138}$$

Oshikawa and Affleck have considered the converse problem of expressing tensor products of Ising boundary states as linear combinations of orbifold boundary states. Their results confirm our conclusion that $|B)$ goes over to a projector on the ferromagnetic ground space [38], i.e, the two Schmidt vectors correspond to fixing all spins up at the cut or all spins down. Referring again to the Dirichlet boundary state of the free-boson *Eq.* (94), Oshikawa and Affleck find that,

$$|D(\phi = 0)) = \frac{1}{\sqrt{2}}\left[|\uparrow)|\uparrow) + |\downarrow)|\downarrow)\right], \tag{139}$$

where $|\uparrow)$ and $|\downarrow)$ are respectively the all-up and all-down states of the Ising Hilbert space. The state $|D(\phi = 0))$ pins the interaction potential in the action defined by Eq. (138) at the minimal value. It is therefore the Dirichlet boundary state that maximizes $(D(\phi)|B)$, and thus the IR fixed point of $|B)$. Under the mapping from operators to states,

$$|\uparrow)|\uparrow) + |\downarrow)|\downarrow) \mapsto |\uparrow)(\uparrow| + |\downarrow)(\downarrow|, \tag{140}$$

and hence the entanglement spectrum is degenerate.

Let the two states spanning the groundspace of the entanglement Hamiltonian be denoted $|\Psi_\uparrow\rangle$ and $|\Psi_\downarrow\rangle$. Chapter 4 yields the following expressions for these states (of the non-traced-over degrees of freedom):

$$\langle\{\mathbf{x}_i\}_{i\leq n} \mid \Psi_\uparrow\rangle := \mu^n \langle 0|\, \sigma(\mathbf{x}_1)\ldots\sigma(\mathbf{x}_n)\, |\uparrow\rangle, \tag{141}$$

$$\langle \{\mathbf{x}_i\}_{i\leq n} \mid \Psi_\downarrow \rangle := \mu^n \langle 0| \sigma(\mathbf{x}_1) \dots \sigma(\mathbf{x}_n) |\downarrow\rangle , \tag{142}$$

where $|0\rangle$ is the groundstate of the critical Ising model, and $|\uparrow\rangle, |\downarrow\rangle$ are the CFT boundary states corresponding to all spins up and all spins down. Odd numbers of particles enter with opposite signs in the expressions for $|\Psi_\uparrow\rangle$ and $|\Psi_\downarrow\rangle$ and so their linear combinations describe orthogonal particle-number-parity sectors,

$$|\Psi_{\text{even}}\rangle := \frac{1}{2}\left(|\Psi_\uparrow\rangle + |\Psi_\downarrow\rangle\right) \tag{143}$$

$$|\Psi_{\text{odd}}\rangle := \frac{1}{2}\left(|\Psi_\uparrow\rangle - |\Psi_\downarrow\rangle\right). \tag{144}$$

Particle parity cannot be enforced without non-local entanglement, and so the density matrix describes a statistical ensemble of two, orthogonal, non-locally entangled states.

It is perhaps surprising that the entanglement spectrum of the Ising-Spin Spin-MR State does not resemble the spectrum of the critical Ising model, but instead the energy spectrum of the ferromagnetic fixed-point model. The ferromagnetic fixed-point model is also a CFT, but a non-local one. This result is to be expected if the same continuum $|\Psi\rangle$ is the limit of the state constructed by taking a trivial product state wavefuncion and projecting out the parity-odd components. We could have then defined $|\Psi\rangle$ in terms of the ferromagnetic fixed point CFT and observed that the entanglement spectrum corresponded to the CFT spectrum. This example suggests that — because of charge screening — long-range features of a Spin-MR State are not sensitive to the choice of CFT made in the ansatz, meaning that any one-to-one correspondence between entanglement and CFT spectrum is not universally accessible in the IR.

6 Conclusion

Condensed matter theory studies systems of many degrees of freedom. Descriptions of these systems that are physically realistic in their microscopic detail tend, by virtue of that same detail, to be analytically intractable. A key insight of the discipline is that important macroscopic observables are insensitive to microscopic details. That is, some macroscopic behavior is *universal*, in the sense that it is common to a set, a *universality class*, of variegated microscopic descriptions. Hence, to develop a theory of the macroscopic behavior of a universality class, a tractable strategy is to choose a mathematically simple representative of the universality class and investigate what macroscopic behavior this caricature predicts. This strategy was followed by Laughlin in his Nobel-prize winning explanation of the integer quantum-hall effect, and by Moore and Read in their seminal treatment of fractional quantum-hall states.

This thesis has followed the same strategy, towards better understanding a family of universality classes of quantum systems: symmetry protected topological order (SPT). SPT order is the generalization to interacting systems of topological band insulators. SPT thus stands in relation to topological band insulators just as the fractional quantum hall effect stands in relation to the integer effect. The suggestion motivating this thesis is that, just as the Moore-Read (MR) wavefunction for interacting fermions exhibits topological order, an analogous wavefuction for bosonic excitations of a 2D spin-lattice should exhibit symmetry protected topological order. Such a Spin MR wavefunction equates (left-hand-side) the first quantized amplitude to find a given configuration of n quasi-particles with (right-hand-side) the n point correlation function of a field operator in a 2D Conformal Field Theory (CFT). The right-hand-side has a natural interpretation as a tensor network. The tensor network description shows a holographic equivalence between the Spin MR state – a description of a stationary system in two-spatial dimensions – and a dynamic theory of the boundary degrees of freedom. The original contribution of this thesis has been to derive this equivalence and show how it simplifies calculating the properties of Spin MR states.

Chapter 3 deduced a bulk-boundary dictionary that in Chapter 4 was put to use in developing an algorithm that exploits the holographic equivalence to compute the bipartite entanglement spectrum of Spin MR states. A unique lowest eigenvalue with a macroscopic energy gap to the first excitation is characteristic of trivial SPT-order, and hence a degenerate or gapless spectrum is a signature of non-trivial SPT order. The algorithm, in tensor network language, turns the network on its side and interprets the bulk as an evolution operator acting on the boundary. This reinterpretation is available to any tensor network, but Spin-MR states are special in that the Hamiltonian of the boundary-evolution operator is expressible in terms of the CFT operator that defines the Spin-MR state. Fixed point analysis of this Hamiltonian yields the reduced density matrix of the Spin-MR state on a bipartition via an isomorphism between states ($|X\rangle \otimes |X\rangle$) and operators ($|X\rangle \otimes \langle X|$).

Calculation of the fixed point of the boundary-picture Hamiltonian can be carried out numerically, or approximated analytically using the methods of Boundary CFT. Chapter 5 applied Boundary CFT in this way to one of the as yet rare examples of an SPT state that Scaffidi and Ringel (SR) showed (on numerical grounds) to be expressible as a Spin MR state. The chapter showed that the reduced density matrix on a bipartition commuted with a representation of the Virasoro algebra, with the implication that its spectrum is highly degenerate, as predicted. Chapter 5 also applied Boundary CFT to compute the entanglement spectrum of a Spin-MR State constructed out of the critical Ising model. The reduced density matrix that results is a projector onto the ground-space of the ferromagnetic model; hence, the entanglement spectrum is low-rank degenerate in this case. The Ising-model example suggests that the long-range features of a Spin-MR state do not depend on the exact choice of auxiliary CFT. These details are plausibly hidden at long-ranges because the particle ensemble is in a charge-screening phase. It follows that a one-to-one correspondence between auxiliary CFT spectra and entanglement spectra does not obtain in general.

The analytical approximations developed in this thesis are exact in the limit that the particle ensemble described by the Spin-MR wavefunction is both vanishingly rarefied on the lattice scale and infinitely dense on the scale of the total system size. Its analytic treatment provides a launching point for further numerical investigations of Spin-MR States on finite-sized lattices.

References

[1] Bela Bauer, Guifre Vidal, and Matthias Troyer. Assessing the accuracy of projected entangled-pair states on infinite lattices. *Journal of Statistical Mechanics: Theory and Experiment*, 2009(09):P09006, 2009.

[2] Denis Bernard and Andre Leclair. Residual quantum symmetries of the restricted sine-gordon theories. *Nuclear Physics B*, 340(2):721–751, 1990.

[3] B Andrei Bernevig and Taylor L Hughes. *Topological insulators and topological superconductors*. Princeton university press, 2013.

[4] Daniel Boyanovsky. Field theory of the two-dimensional ising model: Conformal invariance, order and disorder, and bosonization. *Physical Review B*, 39(10):6744, 1989.

[5] Jacob C Bridgeman and Christopher T Chubb. Hand-waving and interpretive dance: An introductory course on tensor networks. *arXiv preprint arXiv:1603.03039*, 2016.

[6] Nick Bultinck, Robijn Vanhove, Jutho Haegeman, and Frank Verstraete. Global anomaly detection in two-dimensional symmetry-protected topological phases. *Physical review letters*, 120(15):156601, 2018.

[7] John Cardy. Boundary conformal field theory. *arXiv preprint hep-th/0411189*, 2004.

[8] John Cardy. Bulk renormalization group flows and boundary states in conformal field theories. *SciPost Physics*, 3(2):011, 2017.

[9] John L Cardy. Boundary conditions, fusion rules and the verlinde formula. *Nuclear Physics B*, 324(3):581–596, 1989.

[10] Xie Chen, Zheng-Cheng Gu, Zheng-Xin Liu, and Xiao-Gang Wen. Symmetry-protected topological orders in interacting bosonic systems. *Science*, 338(6114):1604–1606, 2012.

[11] Xie Chen, Zheng-Cheng Gu, Zheng-Xin Liu, and Xiao-Gang Wen. Symmetry protected topological orders and the group cohomology of their symmetry group. *Physical Review B*, 87(15):155114, 2013.

[12] J Ignacio Cirac, Didier Poilblanc, Norbert Schuch, and Frank Verstraete. Entanglement spectrum and boundary theories with projected entangled-pair states. *Physical Review B*, 83(24):245134, 2011.

[13] Ph Di Francesco, H Saleur, and JB Zuber. Critical ising correlation functions in the plane and on the torus. *Nuclear Physics B*, 290:527–581, 1987.

[14] Robbert Dijkgraaf, Cumrun Vafa, Erik Verlinde, and Herman Verlinde. The operator algebra of orbifold models. *Communications in Mathematical Physics*, 123(3):485–526, 1989.

[15] J Dubail, N Read, and EH Rezayi. Edge-state inner products and real-space entanglement spectrum of trial quantum hall states. *Physical Review B*, 86(24):245310, 2012.

[16] Glen Evenbly and Guifre Vidal. Tensor network renormalization. *Physical review letters*, 115(18):180405, 2015.

[17] Glen Evenbly and Guifre Vidal. Tensor network renormalization yields the multiscale entanglement renormalization ansatz. *Physical review letters*, 115(20):200401, 2015.

[18] Steven T Flammia, Alioscia Hamma, Taylor L Hughes, and Xiao-Gang Wen. Topological entanglement rényi entropy and reduced density matrix structure. *Physical review letters*, 103(26):261601, 2009.

[19] Philippe Francesco, Pierre Mathieu, and David Sénéchal. *Conformal field theory*. Springer Science & Business Media, 2012.

[20] Ivan Glasser, J Ignacio Cirac, Germán Sierra, and Anne EB Nielsen. Exact parent hamiltonians of bosonic and fermionic moore–read states on lattices and local models. *New Journal of Physics*, 17(8):082001, 2015.

[21] Alexander O Gogolin, Alexander A Nersesyan, and Alexei M Tsvelik. *Bosonization and strongly correlated systems*. Cambridge University Press, 2004.

[22] Bo Han, Apoorv Tiwari, Chang-Tse Hsieh, and Shinsei Ryu. Boundary conformal field theory and symmetry-protected topological phases in 2+ 1 dimensions. *Physical Review B*, 96(12):125105, 2017.

[23] Ching-Yu Huang and Tzu-Chieh Wei. Detecting and identifying two-dimensional symmetry-protected topological, symmetry-breaking, and intrinsic topological phases with modular matrices via tensor-network methods. *Physical Review B*, 93(15):155163, 2016.

[24] Claude Itzykson, Hubert Saleur, and Jean-Bernard Zuber. *Conformal invariance and applications to statistical mechanics*. World Scientific, 1988.

[25] David Jennings, Christoph Brockt, Jutho Haegeman, Tobias J Osborne, and Frank Verstraete. Continuum tensor network field states, path integral representations and spatial symmetries. *New Journal of Physics*, 17(6):063039, 2015.

[26] V Kalmeyer and RB Laughlin. Equivalence of the resonating-valence-bond and fractional quantum hall states. *Physical Review Letters*, 59(18):2095, 1987.

[27] Anton Kapustin, Alex Turzillo, and Minyoung You. Topological field theory and matrix product states. *Physical Review B*, 96(7):075125, 2017.

[28] John Michael Kosterlitz and David James Thouless. Ordering, metastability and phase transitions in two-dimensional systems. *Journal of Physics C: Solid State Physics*, 6(7):1181, 1973.

[29] Michael Levin and Zheng-Cheng Gu. Braiding statistics approach to symmetry-protected topological phases. *Physical Review B*, 86(11):115109, 2012.

[30] Hui Li and F Duncan M Haldane. Entanglement spectrum as a generalization of entanglement entropy: Identification of topological order in non-abelian fractional quantum hall effect states. *Physical review letters*, 101(1):010504, 2008.

[31] Michael Lubasch, J Ignacio Cirac, and Mari-Carmen Banuls. Algorithms for finite projected entangled pair states. *Physical Review B*, 90(6):064425, 2014.

[32] Shohei Miyakoshi, Satoshi Nishimoto, and Yukinori Ohta. Entanglement properties of the haldane phases: A finite system-size approach. *Physical Review B*, 94(23):235155, 2016.

[33] Gregory Moore and Nicholas Read. Nonabelions in the fractional quantum hall effect. *Nuclear Physics B*, 360(2-3):362–396, 1991.

[34] Anne EB Nielsen, J Ignacio Cirac, and Germán Sierra. Laughlin spin-liquid states on lattices obtained from conformal field theory. *Physical review letters*, 108(25):257206, 2012.

[35] Román Orús. Exploring corner transfer matrices and corner tensors for the classical simulation of quantum lattice systems. *Physical Review B*, 85(20):205117, 2012.

[36] Román Orús. Advances on tensor network theory: symmetries, fermions, entanglement, and holography. *The European Physical Journal B*, 87(11):280, 2014.

[37] Masaki Oshikawa and Ian Affleck. Defect lines in the ising model and boundary states on orbifolds. *Physical review letters*, 77(13):2604, 1996.

[38] Masaki Oshikawa and Ian Affleck. Boundary conformal field theory approach to the critical two-dimensional ising model with a defect line. *Nuclear Physics B*, 495(3):533–582, 1997.

[39] Askold Perelomov. *Generalized coherent states and their applications*. Springer Science & Business Media, 2012.

[40] Subir Sachdev. *Quantum phase transitions*. Cambridge university press, 2011.

[41] Thomas Scaffidi and Zohar Ringel. Wave functions of symmetry-protected topological phases from conformal field theories. *Physical Review B*, 93(11):115105, 2016.

[42] Ulrich Schollwöck. The density-matrix renormalization group in the age of matrix product states. *Annals of Physics*, 326(1):96–192, 2011.

[43] R Shankar and Ashvin Vishwanath. Equality of bulk wave functions and edge correlations in some topological superconductors: A spacetime derivation. *Physical review letters*, 107(10):106803, 2011.

[44] Sei Suzuki, Jun-ichi Inoue, and Bikas K Chakrabarti. *Quantum Ising phases and transitions in transverse Ising models*, volume 862. Springer, 2012.

[45] Frank Verstraete, Valentin Murg, and J Ignacio Cirac. Matrix product states, projected entangled pair states, and variational renormalization group methods for quantum spin systems. *Advances in Physics*, 57(2):143–224, 2008.

[46] Frank Verstraete, Michael M Wolf, David Perez-Garcia, and J Ignacio Cirac. Criticality, the area law, and the computational power of projected entangled pair states. *Physical review letters*, 96(22):220601, 2006.

[47] Guifré Vidal. Class of quantum many-body states that can be efficiently simulated. *Physical review letters*, 101(11):110501, 2008.

[48] Xiao-Gang Wen. *Quantum field theory of many-body systems: from the origin of sound to an origin of light and electrons*. Oxford University Press on Demand, 2004.

[49] Keola Wierschem and Pinaki Sengupta. Strange correlations in spin-1 heisenberg antiferromagnets. *Physical Review B*, 90(11):115157, 2014.

[50] Dominic J Williamson, Nick Bultinck, Michael Mariën, Mehmet B Şahinoğlu, Jutho Haegeman, and Frank Verstraete. Matrix product operators for symmetry-protected topological phases: Gauging and edge theories. *Physical Review B*, 94(20):205150, 2016.

[51] Han-Qing Wu, Yuan-Yao He, Yi-Zhuang You, Cenke Xu, Zi Yang Meng, and Zhong-Yi Lu. Quantum monte carlo study of strange correlator in interacting topological insulators. *Physical Review B*, 92(16):165123, 2015.

[52] Yi-Zhuang You, Zhen Bi, Alex Rasmussen, Kevin Slagle, and Cenke Xu. Wave function and strange correlator of short-range entangled states. *Physical review letters*, 112(24):247202, 2014.

[53] Michael P Zaletel and Roger SK Mong. Exact matrix product states for quantum hall wave functions. *Physical Review B*, 86(24):245305, 2012.

[54] Haijun Zhang, Chao-Xing Liu, Xiao-Liang Qi, Xi Dai, Zhong Fang, and Shou-Cheng Zhang. Topological insulators in bi 2 se 3, bi 2 te 3 and sb 2 te 3 with a single dirac cone on the surface. *Nature physics*, 5(6):438, 2009.